

THE DEPENDENCE OF MECHANICAL CHARACTERISTICS
OF WASPALOY AT 1000° - 1400°F
ON THE GAMMA PRIME PHASE
CASE FILE
COPY

by

David J. Wilson and James W. Freeman

THE UNIVERSITY OF MICHIGAN
College of Engineering
Department of Chemical and Metallurgical Engineering

prepared for

NATIONAL AERONAUTICS AND SPACE ADMINISTRATION

NASA Lewis Research Center
Contract NSL-23-005-005
John C. Freche, Project Manager

NOTICE

This report was prepared as an account of Government-sponsored work. Neither the United States, nor the National Aeronautics and Space Administration (NASA), nor any person acting on behalf of NASA:

- A.) Makes any warranty or representation, expressed or implied, with respect to the accuracy, completeness, or usefulness of the information contained in this report, or that the use of any information, apparatus, method, or process disclosed in this report may not infringe privately-owned rights; or
- B.) Assumes any liabilities with respect to the use of, or for damages resulting from the use of, any information, apparatus, method or process disclosed in this report.

As used above, "person acting on behalf of NASA" includes any employee or contractor of NASA, or employee of such contractor, to the extent that such employee or contractor of NASA or employee of such contractor prepares, disseminates, or provides access to any information pursuant to his employment or contract with NASA, or his employment with such contractor.

PERIODIC REPORT

THE DEPENDENCE OF MECHANICAL CHARACTERISTICS
OF WASPALOY AT 1000° - 1400°F
ON THE GAMMA PRIME PHASE

by

David J. Wilson and James W. Freeman

THE UNIVERSITY OF MICHIGAN
College of Engineering
Department of Chemical and Metallurgical Engineering

prepared for

NATIONAL AERONAUTICS AND SPACE ADMINISTRATION

October 1, 1969

CONTRACT NSL-23-005-005

NASA Lewis Research Center
Cleveland, Ohio
John C. Freche, Project Manager
Fatigue and Alloys Research Branch

ABSTRACT

The tensile and creep-rupture properties of Waspaloy at 1000° to 1400°F were correlated with the nature of the interactions of the dislocations with the gamma prime particles. The dislocation mechanism varied from shearing of fine γ' particles to by-passing the larger particles. The study was limited to unnotched specimens although the ultimate objective of the investigation is to clarify the time dependent notch-weakening of nickel base sheet superalloys in the temperature range of 1000° to 1200°F.

TABLE OF CONTENTS

	<u>Page</u>
Introduction	1
Experimental Procedures	2
Tensile and Creep-Rupture Properties	4
Short-Time Tensile Properties	4
Rupture Properties	5
Minimum Creep Rates	5
Deformation in Creep-Rupture Tests	6
Microstructures and Fracture Mechanisms	8
Original Materials	8
Fractured Specimen Characteristics	10
Fracture Sequence	11
Phase Reactions Occurring During Testing.	12
Dislocation Mechanisms	13
Discussion	16
Relationship of Ductility to the Dislocation Mechanism	16
Strength Characteristics	19
Additional Factors	21
Conclusions	22
References	24
Tables	26
Figures	28

LIST OF FIGURES

<u>Figure</u>	<u>Page</u>
1. Smooth (unnotched Specimen).	28
2. Smooth specimen tensile properties from 1000° - 1400°F for 0.026-inch thick Waspaloy sheet heat treated 1/2 hour at 1975°F and aged 16 hours at 1400°F or 10 hours at 1700°F	29
3. Stress versus rupture time data obtained from smooth specimens of 0.026-inch thick Waspaloy sheet heat treated 1/2 hour at 1975°F and aged	30
4. Time-temperature dependence of the rupture strengths at 1000° - 1400°F of smooth specimens of 0.026-inch thick Waspaloy sheet heat treated 1/2 hour at 1975°F and aged 16 hours at 1400°F or 10 hours at 1700°F	31
5. Stress versus minimum creep rate at 1000° - 1400°F for 0.026-inch thick Waspaloy sheet heat treated 1/2 hour at 1975°F and aged at 1400°F or 1700°F	32
6. Stress versus minimum creep rates temperature compen- sated to 1000°F from tests at 1000° - 1400°F for 0.026- inch thick Waspaloy sheet heat treated 1/2 hour at 1975°F and aged 16 hours at 1400°F or 10 hours at 1700°F	33
7. Elongation at fracture versus stress for tensile and rupture tests at 1000° - 1400°F for 0.026-inch thick Waspaloy sheet heat treated 1/2 hour at 1975°F and aged 16 hours at 1400°F or 10 hours at 1700°F	34
8. Selected creep curves obtained at 1000° - 1400°F for 0.026- inch thick Waspaloy sheet heat treated 1/2 hour at 1975°F and aged 16 hours at 1400°F	35
9. Selected creep curves obtained at 1000° - 1400°F for 0.026- inch thick Waspaloy sheet heat treated 1/2 hour at 1975°F and aged 10 hours at 1700°F	36
10. Photomicrographs of 0.026-inch thick Waspaloy sheet heat treated 1/2 hour at 1975°F and aged	37

<u>Figure</u>	<u>Page</u>
11. Intergranular crack length versus initial loading stress at 1000° - 1400°F obtained from fractured tensile and rupture tested smooth specimens of 0.026-inch thick Waspaloy sheet heat treated 1/2 hour at 1975°F and aged 16 hours at 1400°F or 10 hours at 1700°F	38
12. Transmission electron micrographs of Waspaloy, heat treated 1/2 hour at 1975°F, aged, and creep rupture tested at 38 ksi at 1400°F	39
13. Thin-foil electron micrographs of Waspaloy, heat treated 1/2 hour at 1975°F, aged 16 hours at 1400°F, and tensile tested at 1000°F.	40
14. Thin-foil electron micrographs of Waspaloy, heat treated 1/2 hour at 1975°F, aged 16 hours at 1400°F, and creep-rupture tested at 135 ksi at 1000°F	41
15. Transmission electron micrographs of Waspaloy, heat treated 1/2 hour at 1975°F, aged 16 hours at 1400°F and strained 2.3% at 1000°F	42
16. Thin-foil electron micrographs of Waspaloy, heat treated 1/2 hour at 1975°F, aged 16 hours at 1400°F and creep rupture tested at 1200° and 1300°F	43
17. Thin-foil electron micrographs of Waspaloy, heat treated 1/2 hour at 1975°F, aged 16 hours at 1400°F and tensile tested at 1400°F.	44
18. Transmission electron micrographs of Waspaloy, heat treated 1/2 hour at 1975°F, aged 16 hours at 1400°F and creep-rupture tested at 38 ksi at 1400°F	45
19. Transmission electron micrographs of Waspaloy, heat treated 1/2 hour at 1975°F, aged 10 hours at 1700°F and tensile tested at 1000°F	46
20. Thin-foil electron micrographs of Waspaloy, heat treated 1/2 hour at 1975°F, aged 10 hours at 1700°F and strained approximately 1, 2.5, and 6% at 1000°F	47

<u>Figure</u>		<u>Page</u>
21.	Thin-foil electron micrographs of Waspaloy, heat treated 1/2 hour at 1975°F, aged 10 hours at 1700°F and creep-rupture tested at 1000° and 1200°F.	48
22.	Thin-foil electron micrographs of Waspaloy, heat treated 1/2 hour at 1975°F, aged 10 hours at 1700°F and tensile tested at 1400°F	49
23.	Transmission electron micrographs of Waspaloy, heat treated 1/2 hour at 1975°F, aged 10 hours at 1700°F and creep-rupture tested at 38 ksi at 1400°F	50

SUMMARY

The study carried out was designed to enable correlations to be established between the nature of deformation leading to fracture and the tensile and creep-rupture properties at 1000° - 1400°F for two widely different γ' particle sizes in a nickel base superalloy. The relationships established for smooth specimens will be extended in future research to enable the determination of the cause of the severe time dependent, edge-notch sensitivity that can occur for the sheet alloys exposed under creep-rupture conditions at 1000° and 1200°F (refs. 1, 2, 3, 4). Waspaloy sheet, solution treated at 1975°F and aged 16 hours at 1400° in one case and 10 hours at 1700°F in the other, were utilized to obtain the variation in γ' particle size.

The results demonstrated that deformation occurred by dislocation mechanisms which were dependent on the γ' particle size. Dislocations sheared γ' particles smaller than a critical size, whereas larger particles were by-passed. Corresponding to the changes in the nature of the interactions of the dislocations with the γ' phase, variations in tensile and creep-rupture properties occurred. The deformation was homogeneous when the γ' particles were by-passed by the dislocation and led to higher elongations than for the localized deformation that occurred when the γ' particles were sheared by the dislocations. The critical resolved shear stress increases for increasing γ' size below the critical and decreases for increasing size above the critical. Based on the variations in mechanical characteristics with the γ' size relative to the critical size techniques are suggested for arriving at optimum properties.

INTRODUCTION

Results are presented that were obtained as an integral part of a current investigation being carried out to determine the scope and cause of the severe time-dependent edge-notch sensitivity of nickel-base superalloy sheet materials at 1000° and 1200°F. The research was carried out at the University of Michigan, Ann Arbor, Michigan, under sponsorship of the National Aeronautics and Space Administration, Washington, D. C.

Studies carried out to date (refs. 1, 2, 3, 4) have to a great extent established the scope of the problem and, perhaps more important, created a general awareness of the importance and potential dangers associated with the phenomenon to design and materials engineers. The experiments reported represent the research that is being carried out to establish the basic mechanisms or phenomena that cause the notch sensitive behavior.

It has been demonstrated (refs. 3, 4) that failure of both smooth and notch creep-rupture specimens occurs by intergranular crack initiation and growth (apparently by creep) until abrupt shear occurs due to the increase in stress resulting from the reduction in load-carrying area. In addition, it is apparent that the notch sensitivity is determined primarily by the time periods for the first stages of intergranular cracking. The deformation characteristics of the materials, particularly as they are related to intergranular crack initiation, are, therefore, of prime importance in the occurrence of notch sensitive behavior.

In the early studies it was also shown that the degree of the notch sensitivity varied considerably with the heat treatment, particularly the aging treatment of the alloys (refs. 3, 4). In addition, the variation in heat treatment resulted in changes in microstructural features, mechanical characteristics, deformation and fracture behavior. The present study was based on the concept that the establishment of the interrelationships between the above factors would provide an understanding of the cause of

the notch sensitivity. Particular emphasis has been placed on the relationships between the various factors and the dislocation mechanisms operative in the alloys. For simplicity the dislocation study has been up to the present time confined to the investigation of smooth specimens. It is believed, however, that notch specimen behavior can be related to that of the smooth specimens.

The mechanical behavior of Waspaloy, the alloy selected for the investigation, is strongly dependent on the fine dispersion of the γ' phase, $\text{Ni}_3(\text{Al}, \text{Ti})$ present in the aged alloy. The heat treatments chosen for study were those previously used which resulted in distinct γ' size differences and a corresponding large variation in notch sensitivity (ref. 3). Tensile and creep rupture tests were carried out in the temperature range where severe time dependent notch sensitivity can occur ($1000^\circ - 1200^\circ\text{F}$). In addition, testing was carried out at higher temperatures (up to 1400°F) in order to provide a contrasting case where the notch sensitivity has not been observed. The microstructural features, particularly the dislocation substructures present in the tested specimens, were evaluated.

EXPERIMENTAL PROCEDURES

The commercially produced Waspaloy used in the investigation had the following reported chemical composition (weight per cent):

<u>Ni</u>	<u>Cr</u>	<u>Co</u>	<u>Mo</u>	<u>Ti</u>	<u>Al</u>	<u>C</u>	<u>B</u>	<u>Zr</u>	<u>Fe</u>	<u>S</u>
Bal	19.33	13.32	4.16	2.95	1.35	0.06	0.005	0.03	0.55	0.007
				<u>Mn</u>	<u>Si</u>	<u>Cu</u>				
				<0.01	0.05	0.03				

The material was received as 0.026-inch thick sheet cold worked 23 - 25 per cent. Specimen blanks were cut in the longitudinal direction prior to heat treatment.

The heat treatments consisted of a solution treatment followed by a lower temperature aging treatment. The solution treatment of 1/2 hour at 1975°F was carried out on each specimen blank in an argon atmosphere. Subsequent air-cooling was rapid enough to sufficiently suppress γ' precipitation so that the particle size could be controlled by subsequent aging treatments. The two separate aging treatments utilized, 16 hours at 1400°F, air cooled, and 10 hours at 1700°F, air cooled, were carried out in batches of ten or twelve blanks. The aging treatments were designed to produce γ' particles whose average size would vary by an order of magnitude. The combination of the solution treatment at 1975°F and aging at 1400°F was also adequately representative of industrial practice.

After heat treatment, blanks were machined into smooth specimens (fig. 1). Tensile tests were conducted at a cross head speed of approximately 0.01-inch per minute up to about 2 per cent deformation. The strain rate was then increased to about 0.05-inch per minute until failure. The creep-rupture tests were conducted in beam-loaded machines in accordance with ASTM Recommended Procedures. Specimen rupture times were recorded automatically. Creep was measured by an optical system, which had a sensitivity of five-millionths of an inch.

The study of the structures was carried out by conventional methods employed for microstructural examination. Samples for optical microscopy and replica electron microscopy were etched electrolytically in "G" etch, an etchant developed by Bigelow et al (ref. 5). Samples approximately 0.5-inches wide by 0.7-inches long for transmission electron microscopy of the tested specimens were cut from the gauge lengths about 0.5-inch from the fractures. Thinning of samples was accomplished by grinding on wet silicon carbide papers followed by electropolishing. This was carried out at an applied voltage of 35 volts, a current density of 0.5 amps/cm (ref. 2), in conjunction with a

chilled mixture of 6 per cent perchloric acid and 94 per cent acetic acid. The thin films were studied and photomicrographed in a JEM electron microscope operated at 100KV.

TENSILE AND CREEP-RUPTURE PROPERTIES

Tensile and creep-rupture properties were established in the temperature range of 1000° - 1400°F for Waspaloy sheet solution treated at 1975°F and aged 16 hours at 1400°F in one case and 10 hours at 1700°F in the other.

Short-Time Tensile Properties

The tensile test results (table 1, figure 2) exhibited the following:

- (1) The tensile and yield strengths were lower after aging at 1700°F than for aging at 1400°F.
- (2) The tensile strengths were considerably lower at 1400°F than at 1000° and 1200°F. The yield strength, for the material aged at 1400°F, exhibited some decrease from increasing the testing temperature from 1000° to 1400°F. The yield strength was essentially constant from 1000° to 1400°F after aging at 1700°F. The ratios of YS/TS were higher at 1400°F than at 1000° or 1200°F.
- (3) The elongation and reduction of area values were higher at 1200° and 1400°F after aging at 1700°F than for the material aged at 1400°F.
- (4) Most noticeable was the decreasing elongation values with increasing temperature, particularly for the material aged at 1400°F for which the value fell from 30 per cent at 1000°F to 6 per cent at 1400°F. The reduction in area values showed less decrease than the elongation with increasing temperature.

Rupture Properties

The rupture data are presented in table 2 and as stress-rupture time curves in figure 3. In addition, the data were parameterized using the Larson-Miller parameter (ref. 6) with an assumed constant C of 20 (fig. 4). The rupture curves had slight slopes at 1000° and 1100°F with steeper slopes at 1300° and 1400°F. At 1200°F, the rupture curve for the material aged at 1400°F exhibited an apparent instability (nature of the curve derived by the "family-of-curves concept"). For the material aged at 1700°F, the curve at 1200°F had a relatively low gradient.

Most apparent from the parameterized data (fig. 4) was that at the lower stresses the strength levels of the materials aged at 1400° and at 1700°F were similar. This occurred even though, as it is later shown in subsequent sections, the two heat treated materials clearly exhibited different deformation characteristics. At high stress levels aging at 1400°F resulted in higher rupture strengths than aging at 1700°F.

It is evident from the parameter curves that the rupture data consists of two distinct regimes which differ significantly in slope. Moreover, it appears that the change in behavior from the high stress to the low stress regimes occurs as the stress is reduced below the approximate 0.2 per cent offset yield strength. The slopes of the regimes in the parameter curves are directly reflective of the variations in slopes previously presented for the stress-rupture time curves.

Minimum Creep Rates

All of the tests were instrumented to measure creep. The minimum creep rates (table 2) are plotted as stress-creep rate curves in figure 5. The changes in slope of the curves with temperature are analogous to those previously described for the stress-rupture time curves.

As a method of comparing the creep resistance of the two heat treated materials and clarifying changes in creep resistance with stress,

temperature compensated creep rates were determined by correcting all the values to 1000°F (fig. 6). To accomplish this, the following relationship was used:

$$\dot{\epsilon}_1 e^{\frac{\Delta H}{RT_1}} = \dot{\epsilon}_2 e^{\frac{\Delta H}{RT_2}}$$

where: $\dot{\epsilon}$ = Minimum creep rate

ΔH = Apparent activation energy for creep

T = Absolute temperature

R = Gas constant

The value of 133,000 cal/mole, reported by A. Webster and B. J. Piercey for the Ni-base superalloy Mar-M200 (ref. 7), was used for the apparent activation energy for creep. This value is approximately twice the activation energy for diffusion. The applicability of this value is evident from the agreement in the temperature compensated creep rates which were derived from tests at different temperatures but at the same stress levels. Like the rupture characteristics, two distinct regimes are evident with changes of slope of the curves at about the 0.2 per cent offset yield strengths. The stress exponents (n in the relationship $\dot{\epsilon} = A \sigma^n$) for the high and low stress regimes are approximately 30 and 7 respectively. It was evident that, even at the lower stress levels, somewhat higher minimum creep rates resulted from aging at 1700°F than aging at 1400°F.

Deformation in Creep-Rupture Tests

The ductility in rupture tests varied considerably with the test conditions (temperature and stress) as well as the aging treatment (table 2). For the material aged at 1400°F, the rupture elongation decreased with time at 1000° and 1100°F, decreased and subsequently increased with time at 1200°F, and increased with time at 1300° and 1400°F.

The elongation values were plotted as a function of stress (fig. 7). This graphical method was used as a means of presenting the data since it permitted easy comparison of the elongations as a function of the test

conditions (stress and temperature) and with heat treatment. The data from the tensile tests are also included in this representation. From this graph it is evident that the elongations for the material aged at 1400°F, as a function of stress, form a trough with a minimum of about 1.5 per cent at approximately 85 ksi.

The elongations of the ruptured specimens of the material aged at 1700°F were considerably higher than those aged at 1400°F (fig. 7). However, the elongations decreased with time at 1000° and 1100°F. For test temperatures from 1200° to 1400°F, the elongations remained at relatively high levels.

The reduction in area values reported (table 2) are the average values across the fractures. Due to the complex nature of the fracture (discussed in a subsequent section), considerable variations in reduction of area occurred along the path of the fracture. The values for both materials decreased until the load was reduced to approximately 110 ksi after which very little change occurred. Aging at 1700°F resulted in somewhat higher values than aging at 1400°F.

The variations in rupture elongation, when correlated as a function of stress level, are reflective of pronounced variations in the amounts of deformation occurring during the individual stages of creep. (Selected creep curves are presented in figs. 8 and 9.) Examination of the contribution of the deformation in the various stages of creep to the total elongation resulted in the following observations:

- (1) As expected, there was a marked increase in the deformation that occurred on application of the load with increasing stress above the yield stress.
- (2) For the materials aged at 1400°F, there was very little deformation in first or second stage of creep. The deformation was very low in third stage creep when the stress was above or near to the yield strength. Accordingly, the elongation fell to low values as the stress was decreased to the approximate yield

strength. However, the deformation in third-stage creep increased as the stress was decreased below the yield strength, i.e., in the higher temperature tests. Consequently, the elongation again increased at the lower stress levels. The result was an "elongation trough" near the yield strength. In other words, the elongation was a minimum when there was little yielding during loading, and the stress was close enough to the yield strength so that there was little third-stage creep.

- (3) For aging at 1700°F the deformation decreased as the stress was reduced towards the yield strength. It did not fall off to such low values as those observed for the material aged at 1400°F because the deformation in third stage creep became high as the stresses fell to and below the yield strength. The contribution to the total elongation from first and second stage creep was relatively small.

MICROSTRUCTURES AND FRACTURE MECHANISMS

The major results of the investigation were obtained by microstructural studies. First, the original structures were categorized and recorded. Second, the fractured specimens were examined particularly to establish the dislocation mechanisms operative.

Original Materials

The microstructures of solution treated and aged Waspaloy essentially consists of the matrix gamma, the gamma prime precipitate, $\text{Ni}_3(\text{Al}, \text{Ti})$, and the two carbides, $\text{Ti}(\text{C}, \text{N})$ and M_{23}C_6 . The object of the heat treatment variations utilized in the present investigation was to alter the γ' particle size and yet to hold the other microstructural features as constant as possible. A single solution treatment at 1975°F used in conjunction with two separate aging treatments (16 hours at 1400°F in one case and 10 hours at 1700°F in the other) were used as a best means to accomplish this. The

following structural features were observed by microscopic examination (fig. 10):

- (1) As a result of utilizing a constant solution treatment, a grain size of 0.020 mm was obtained for the materials aged at either temperature.
- (2) Aging at 1400°F resulted in a dispersion of γ' particles too small to be readily resolvable in the electron microscope using replica techniques (fig. 10b). In the studies using transmission electron microscopy, contrast effects due to the γ' precipitate were observed. The average diameter of these contrast effects was approximately 70 Å. In the diffraction patterns taken from these areas, super-lattice reflections were observed [of the type (100), (110), etc.] which indicated that presence of an ordered precipitate, proof of the presence of γ' precipitate particles.

Aging at 1700°F resulted in larger γ' particles than those produced by the 1400°F treatment. Optical micrographs (fig. 10c) exhibited a mottled appearance within the grains due to the large size of the γ' particles. The degree to which the mottling occurred increased with the severity of the etching. Clearly definable spherical particles were observed in the electron microscope by both replica (fig. 10d) and transmission techniques. In thin foils examined by transmission electromicroscopy, there were contrast effects associated with the γ' precipitate particles which demonstrated their coherent nature (ref. 8). The γ' particles had an average size of about 1000 Å.

- (3) Although there must have been differences in the carbides after the two aging treatments, these were not readily apparent. Quantitative comparisons were difficult because the amounts of the carbide precipitates varied considerably from grain to grain. This was particularly true for the grain boundary precipitate

since variations occurred which were apparently associated with changes at which the plane of the sample intercepted the boundary.

Generally, for both materials, the grain boundaries were partially filled with $M_{23}C_6$ carbide, while the $Ti(C, N)$ was observed as an intragranular globular precipitate. Selected area diffraction and dark field transmission electron microscopy of the grain boundaries showed that the $M_{23}C_6$ carbide had the same orientation as one of the adjacent grains. This orientation relationship was:

$$\begin{array}{ccc} \{100\}_{\gamma} & // & \{100\}_{m_{23}C_6} \\ \langle 100 \rangle_{\gamma} & // & \langle 100 \rangle_{m_{23}C_6} \end{array}$$

This relationship arises since the carbide phase is face centered cubic with a lattice parameter of 10.7 \AA which is almost exactly three times that of the matrix ($a_0 = 3.58 \text{ \AA}$). This situation is identical with that reported for the precipitation of $M_{23}C_6$ in a γ' free austenite (ref. 9).

Fractured Specimen Characteristics

Examination of the specimens after tensile and rupture tests was carried out to determine the deformation and fracture mechanisms that had occurred. Visual and optical microscopy were used to examine the fracture surfaces to establish the mechanisms of the failures. Transmission electron microscopy was carried out, on samples taken somewhat removed from the fracture, to determine the dislocation mechanisms by which the deformation occurred that led to the fractures.

Fracture Sequence

Examination of the failed specimens showed that, for all but a few tensile tests, the fractures consisted of two distinct parts. The fractures, across the specimens, were roughly perpendicular to the edges. One section originated at the edge was perpendicular to the loading axis and tended to be dark in color from oxidation. The remainder of the fracture was not colored from oxidation and was a typical shear fracture, slanted through the thickness. Optical examination showed that these fractures were intergranular and transgranular respectively. These observations indicated that failure of the specimens occurred by initiation and relatively slow growth of the intergranular crack, followed by the shear failure in a time period short enough to avoid discoloration by oxidation. The shear failure occurred when the reduction in cross-sectional area by intergranular cracking raised the stress high enough for the the crack to initiate rapid transgranular failure.

Measurements across the specimen at the fractures showed that greater reduction in thickness occurred in the regions of the transgranular crack than at the intergranular fracture. The reductions in thickness in the two regions progressively became more similar with decreasing loads at the higher temperatures. In the tests at 1400°F, the maximum reduction in thickness at the intergranular fracture was only slightly less than that at the transgranular fracture. The data for the reductions in area in Table 2 are the average values for the reduction in thickness.

In addition to the main intergranular and shear cracks, the majority of the fractured specimens showed the presence of "subsidiary" intergranular cracks. It was evident that the extent of the cracking observed (in the sections parallel to the plane of the sheet specimens) decreased towards the mid-thickness of the specimen.

Within the context of the difficulties involved in estimating the amount of intergranular cracking in the ruptured specimens, the following obser-

ventions (table 2, fig. 11) were made:

- (1) The fractures of the specimens tensile tested at 1000° and 1200°F were entirely transgranular. Part of the fractures were intergranular in the tensile tests at 1400°F. For instance, for the material aged at 1700°F, in the test at 1400°F, 12 per cent of the width of the specimen cracked intergranularly.
- (2) All of the rupture tested specimens exhibited clearly defined intergranular fracture sections. The intergranular crack length increased with decreasing applied loads - i. e., increasing rupture times and test temperatures (fig. 11). This result was to be expected since at the lower applied loads, the intergranular cracks would have to grow to a greater extent before the stress became high enough to initiate the transgranular fracture.
- (3) The amount of intergranular cracking for a given stress was less for the specimens aged at 1700°F than those aged at 1400°F. This occurred because the "transgranular strength," (i. e., the stress on the load bearing section necessary to initiate a transgranular crack) was reduced by increasing the aging temperature from 1400° to 1700°F. For both materials the transgranular strength was reduced by the introduction of the intergranular crack. For example, for the specimen aged at 1400°F, tested at 80 ksi at 1200°F, 34 per cent of the fracture was intergranular. Consequently, the "transgranular strength" was $80 \times 100/66 = 121$ ksi. This value is less than tensile strength at 1200°F of 168 ksi (fracture was entirely transgranular).

Phase Reactions Occurring During Testing

Growth of the γ' precipitate occurred during the creep-rupture tests. This was most pronounced at the higher test temperatures for the material aged 16 hours at 1400°F. During the 1007-hour test at 1400°F, the average size of the γ' increased from about 75Å to 900Å. This may be contrasted to the 931-hour test at 1400°F for the material aged 10 hours at 1700°F,

during which the average size increased from approximately 1000Å to 1500Å.

Denudation of γ' occurred adjacent to the grain boundaries during creep-rupture tests at 1300° and 1400°F. Examples are shown in figure 12. The depletion was not detectably greater on boundaries transverse to the applied stress as was reported by Decker and Freeman (ref. 10). In many cases, the depleted areas occurred on only one side of the boundary (fig. 12b). From electron diffraction patterns and dark field micrographs in the study of the structures using transmission electron microscopy, it was shown that the depleted side was that on which the $M_{23}C_6$ carbide did not have the identical orientation as the adjacent grain.

Dislocation Mechanisms

The mechanical characteristics of Ni-base superalloys hardened with Ti and Al are strongly dependent on the γ' phase and, hence, on the interactions of the dislocations with these particles. Specimens which had been tensile and creep-rupture tested were studied by transmission electron microscopy to establish the dislocation mechanisms by which deformation occurred. The specimens chosen for this detailed examination were selected to encompass the range of test conditions used, i.e., temperature and stress. Therefore, these samples had undergone a wide range in amounts of deformation that led to fracture. (The specimens studied are designated with a * in Table 2.) The only exception was the use of the specimens strained at 1000°F to smaller amounts than necessary for fracture. These specimens were examined since it was not possible to evaluate the dislocation structures present in the specimens tensile tested at 1000°F because of the very extensive deformation that had occurred.

Typical microstructures of the deformed materials are presented in figures 13 - 23. The following observations were made in the study:

(1) Material Aged 16 Hours at 1400°F:

- (a) In the tensile and rupture tests carried out at 1000°F, the stress levels were above the yield strength of the material. The large amounts of the deformation that occurred resulted in extremely high dislocation densities (figs. 13, 14). The dislocations were primarily concentrated on (111) slip planes.

The dislocation mechanism that apparently led to these structures was more readily discernable in the test specimen strained approximately 2 per cent at 1000°F (fig. 15). The superdislocations, i. e., dislocation pairs present in these structures, indicate that moving dislocations shear the precipitate particles. The superdislocation arises since the first whole dislocation disorders the γ' increasing the energy of the particles until the second re-orders them. The presence of stacking faults associated with extended dislocations (fig. 14b) is also proof that the γ' particles are sheared by the dislocations. If they had not sheared but cross slipped around the particles the partial dislocations which constitute the fault would have had to combine.

- (b) The specimens rupture tested at 1200° and 1300°F exhibited relatively low dislocation densities which reflects their low rupture elongation (fig. 16). The dislocations were principally present as pile ups. In a large number of cases the dislocations were dissociated to form stacking fault ribbons.
- (c) The dislocations, in the specimen tensile tested at 1400°F (i. e., tested to stress levels over the yield stress), were concentrated on slip planes (fig. 17) and in some cases dissociated to form stacking faults.
- (d) It was clearly evident in the microstructure of the material rupture tested at 1400°F (at 38 ksi) that γ' growth occurred during the test. The presence of the large γ' led to a

distinctly different dislocation structure than for the previously described cases when the γ' particles were small. The deformation that occurred led to a homogeneous distribution of entangled dislocations (fig. 18a). Gamma prime contrast effects associated with coherency were observed (fig. 18b) demonstrating that at least some of the γ' particles remained coherent even after an overall deformation of 6 per cent.

(2) Material Aged 10 Hours at 1700°F:

- (a) For the material aged at 1700°F, the deformation that had occurred was extremely "general"; the dislocations were homogeneously distributed (figs. 19 - 23). This result for large γ' particles is in strong contrast to the highly localized deformation that occurred when the γ' particles were small, as described for specimens of the material aged at 1400°F (figs. 13 - 17). Even though the γ' particles were large enough to be readily resolvable ($\sim 1000\text{\AA}$), it was difficult to discern the interaction of the dislocations with the particles in the cases where extensive deformation had taken place. In specimens deformed lesser amounts (particularly the specimen strained to a few per cent at 1000°F), it was clear that the dislocation movement occurred by the by-pass mechanism. The dislocations bowed between γ' particles (fig. 20) leaving pinched off dislocation loops. Gamma prime particles that retained their coherency after 9% overall elongation are evident from the contrast effects in figure 23b.

There was evidence that at the high strains developed in the specimen tensile tested at 1000°F of a tendency for the deformation to be concentrated on (111) slip planes (figs. 19 and 20c). It is not clear from the micrographs, however,

whether this effect results from a change in dislocation mechanism from by-passing to shearing the γ' particles.

- (b) The frequency of microtwins (figs. 21a and 22b) was most striking because it was considerably greater than observed in the materials aged at 1400°F. Selected area diffraction patterns were heavily streaked in the $\langle 111 \rangle$ direction which is perpendicular to the planes of the twins. In many cases there appeared to be a higher density of microtwins in the γ' than elsewhere (fig. 22b). This observation would suggest that the γ' had a greater susceptibility to microtwinning than the matrix.

DISCUSSION

Relationship of Ductility to the Dislocation Mechanism

Ductility is a measure of the degree to which a material will deform prior to fracture. Consequently, the nature of the dislocation motion that results in the deformation of the material could be expected to be important to the initiation of cracks leading to fracture. In the material studied, the deformation that occurred subsequent to crack initiation contributed relatively little to the overall elongation. The dislocation mechanisms described previously should, due to the sample location, be typical of the materials just prior to crack initiation and, therefore, typical of the major deformation of the specimens.

In an alloy hardened with a coherent precipitate, dislocations shear particles below a critical size. Particles larger than the critical size are by-passed by the dislocations. G. Luetiering and S. Weissman, in a study of the room tensile properties of age-hardened Ti-Al and Ti-Cu alloys, demonstrated that a correlation existed between particles being sheared by dislocations and low ductility, whereas higher ductility resulted when the dislocations by-passed the precipitate particles (ref. 11). In this investigation, similar correlations occurred for Waspaloy tensile and

creep-rupture tested in the temperature range of 1000° - 1400°F. Aging Waspaloy 16 hours at 1400°F resulted in γ' particles of about 75Å in diameter, which were below the critical size. Thus, in the tests where little or no γ' growth occurred during testing (for example, the tests at 1000° - 1200°F) the dislocations sheared the γ' particles. The ductilities of these tests were significantly lower than those obtained from equivalent tests on the material aged at 1700°F where the γ' particles (approximately 1000Å in diameter) were larger than the critical size and were by-passed by the dislocations. This result is consistent with the concept that "homogeneous" or general deformation (resulting from the by-pass mechanism) leads to ductile behavior. It avoids the high stress concentrations at the head of dislocation pile ups in the more localized deformation (shearing by dislocations) associated with relatively low ductility. A number of additional factors are also evident.

- (1) For the material aged at 1400°F and rupture tested at 1400°F (38 ksi), the γ' particles grew larger than the critical size during the test. The micrographs of the ruptured specimen exhibited a homogeneous distribution of dislocations which indicated that deformation had occurred by the by-pass mechanism. Presumably, if the specimen had been studied for the early part of the test, before the γ' exceeded the critical size, the dislocations present would have been found localized on (111) slip planes, since the deformation would have occurred by the dislocations shearing the precipitate particles.

The test results show an increase in the ductility with increasing rupture time at 1400°F and at long times at 1300°F. Thus, the results indicate that the increases in ductility were due to an increase in the fraction of the rupture time during which the γ' particles exceeded the critical size.

- (2) In the creep-rupture tests at all temperatures and in the tensile tests at 1400°F, failure occurred by intergranular crack initiation and growth followed by transgranular shear. Consequently, intergranular cracks must have been initiated by dislocation motion by both of the observed mechanisms (shearing and by-passing of the γ' particles).

The fractures of the specimens tensile tested at 1000° and 1200°F were entirely transgranular. Presumably, for the material aged at 1400°F, the transgranular cracks originated from the localized deformation that was observed on (111) slip planes. For the specimens aged at 1700°F during the first yielding where the strains were small, dislocation motion clearly occurred by the by-pass mechanism. However, as further yielding occurred and the strain increased, there was evidence that the deformation became, to a certain extent, localized on (111) slip planes, this being consistent with the transgranular fracture mode that occurred.

The fractures of the specimens tensile tested at 1400°F were initiated by intergranular cracks. The material aged at 1700°F exhibited considerably higher elongation than the specimen aged at 1400°F. This result is in accordance with the concept previously presented that the by-pass mechanism leads to higher elongations than when the γ' are sheared by dislocations. Aging at 1700°F prior to tensile tests at 1000° and 1200°F resulted in only slightly greater fracture elongation than aging at 1400°F. All of the specimens failed by transgranular crack initiation. It is suggested that the similarity of the elongations occurs because for both the aged materials the cracks were initiated by excessive slip on (111) planes. Presumably, the slightly higher deformation for the

material aged at 1700°F reflects the fact that at low strains, prior to localized deformation, the dislocations by-pass mechanism was operative. For the material aged at 1400°F, dislocations sheared the γ' particles throughout the tests.

- (3) Elongation of the creep-rupture specimens occurred by deformation on loading (i. e. , at a high strain rate) followed by subsequent creep deformation (i. e. , at a low strain rate). As the loads were reduced to and below the yield strengths, the deformation that occurred on loading decreased markedly. It was also apparent that the tests at the lower temperatures where little or no γ' growth occurred during the tests, the amount of creep deformation that occurred was approximately constant for a given heat treatment. The deformation that occurred during creep for the material aged at 1400°F (1 - 2.5 per cent) was lower than for the material aged at 1700°F (3.5 - 5.5 per cent). These results would tend to suggest that for a fixed γ' size, i. e. , dislocation mechanism, intergranular crack initiation occurred after a fixed amount of creep deformation.

Strength Characteristics

As the γ' size is increased, the critical resolved shear stress for dislocation motion increases until the size exceeds the critical particle size, after which further increase in size results in a decrease in the CRSS (ref. 11). Below and above the critical size, the dislocations shear and by-pass the γ' particles respectively.

The yield strengths were lower after aging at 1700°F than aging at 1400°F. Thus, the particular heat treatments studied were such that shearing occurred in the case of low temperature aged material at a CRSS that was greater than that for the high temperature age where the γ' particles were by-passed by the dislocations.

For the material aged at 1700°F, the yield strength was essentially constant with test temperatures from 1000° - 1400°F. It would be expected to decrease with temperature unless some strengthening mechanism occurred as the test temperature increased. Beardmore et al (ref. 12) demonstrated that this behavior can be attributed to the precipitation of a secondary "hyperfine" distribution of γ' in the matrix γ at temperatures below the aging temperature. The presence of a secondary distribution of fine γ' was not evident in the transmission electron micrographs. However, the results of the tensile tests are consistent with the occurrence of such a precipitation.

The higher the temperature of the aging treatment, the greater the supersaturation of γ' that exists at any given lower temperature. Consequently, while cooling from the aging treatment and during the test exposure, a larger amount of fine γ' could precipitate in the material aged at 1700°F than that aged at 1400°F. The effectiveness of such a fine precipitate in increasing the flow stress would be greater the larger the volume fraction and size of the particles. As the test temperature is increased to the aging temperature, the volume of the secondary precipitate would decrease while the particle size would increase. The combination of these factors could well have resulted in the almost constant flow stress from 1000° to 1400°F for the material aged at 1700°F.

The results for the material aged at 1400°F are also consistent with these concepts since the flow stress decreased somewhat with increasing temperature, particularly as it was increased to the aging temperature at which no secondary fine γ' precipitation should form.

The tensile strengths were lower after aging at 1700°F than for the material aged at 1400°F. Most evident from the results was, however, the drastic decrease in tensile strengths that occurred by increasing the test temperature from 1200° to 1400°F. Corresponding to this decrease, two allied changes occurred.

(1) The tensile tests at 1400°F were clearly initiated by intergranular

cracks while at the lower temperatures, the failures were entirely transgranular.

- (2) The ductilities decreased significantly by increasing temperature from 1000° to 1400°F.

From the rupture tests, it was evident that for both of the aged materials, there was an increase in the slope of the stress-parameter curves as the loads were reduced below the approximate 0.2 per cent offset yield strengths. These instabilities in the curves were not associated with a change from transgranular to intergranular crack initiation since fracture for the tests both above and below the yield stress were initiated by intergranular cracks. Apparently the cause of the behavior also resulted in parallel variations in creep resistance. Although the mechanism has not yet been clarified, it would be safe to assume that the absence of the deformation associated with yielding decreases the resistance to crack initiation.

The equality of the rupture strengths for both aging treatments, when tests were conducted below their yield strengths, was unexpected. The material aged at 1700°F had less creep resistance than the material aged at 1400°F. Apparently, however, the higher deformation to fracture sufficiently increased the rupture times to offset the lower creep resistance. This suggests that the equality of rupture strength was merely coincidental. There were sufficient tests on the material aged at 1400°F, at low enough temperatures, so that it was evident that growth of the γ' particles past the critical size was not responsible for the observed effect.

Additional Factors

As γ' particles increase in size to the critical size, the strength increases due to the greater resistance to shearing by the dislocations. The ductility, however, decreases. When the γ' particle size grows larger than the critical size, dislocations by-pass the γ' and the ductility increases. It is suggested that the best combination of strength and ductility results for γ' particles somewhat larger than the critical size where the strength has

fallen off some from the maximum, but the ductility is higher than for a corresponding strength with sub-critical size γ' . This suggested approach for the development of optimum properties should be applicable, at least at temperatures where the γ' is reasonably stable.

There is also a possibility that multiple aging treatments, commonly applied to superalloys to attain optimum creep-rupture properties (for example, Waspaloy may be aged 24 hours at 1550°F plus 16 hours at 1400°F), may involve both sub-critical and larger than critical γ' particles. On the basis that aging treatments of this type result in a bimodal distribution of γ' , it could be hypothesized that the superior properties are attained due to the following dislocation interactions with the particles:

- (1) The γ' particles larger than the critical size, produced during the high temperature aging treatment, may interact with the dislocation motion to result in homogeneous deformation, and, hence, high ductility.
- (2) At the same time, the fine γ' , formed at the lower aging temperature, presumably should be sheared by the dislocations and act to increase the strength of the alloy.

Consequently, optimum properties, at test temperatures where the γ' is stable, could result because the two types of dislocation motion occur simultaneously.

CONCLUSIONS

The nature of the interactions of dislocations with the γ' phase in Waspaloy was studied to clarify the mechanisms of creep and rupture of Waspaloy sheet at 1000° - 1400°F. The research utilized unnotched specimens with the ultimate objective of clarifying the time dependent edge-notch sensitivity that can occur at 1000° - 1200°F for such alloys under creep-rupture conditions.

- (1) Variations in the γ' size in Waspaloy results in distinctly different dislocation mechanisms by which deformation occurs in tensile and creep-rupture tests at 1000° - 1400°F. Dislocations shear particles smaller than a critical size. Particles larger than the critical size were by-passed by the dislocations, except possibly at high strains.
- (2) Fracture of the creep-rupture specimens at all the test temperatures and the tensile tests at 1400°F occurred by intergranular crack initiation and growth followed by transgranular shear. The latter fracture occurred when the increase in stress on the load bearing area, due to the reduction in area by growth of the intergranular crack, exceeded that necessary to cause rapid shear. The fractures of the tensile specimens tested at 1000° and 1200°F were entirely transgranular.
- (3) The mechanical properties were correlated with the nature of the interactions of the dislocations with the precipitate particles and the fracture mode that occurs. When failure was initiated by dislocation motion by the by-pass mechanism, the homogeneous deformation that occurs resulted in a higher elongation than for the highly localized deformation that results when the γ' particles are sheared by the dislocations. Increasing the size of fine γ' results in an increase in the critical resolved shear stress until the critical size is exceeded, after which it decreases. Consequently, variations in mechanical properties can be related to changes in the γ' particle size relative to the critical size and offer as basis for arriving at aging treatments for optimum properties.

REFERENCES

1. Cullen, T. M., and Freeman, J. W.: The Mechanical Properties at 800°, 1000°, and 1200° of Two Superalloys Under Consideration for Use in the Supersonic Transport. Prepared under Grant No. NsG-124-61 (NASA CR-92) for NASA by The University of Michigan, Ann Arbor, September, 1964.
2. Cullen, T. M., and Freeman, J. W.: The Mechanical Properties of Inconel 718 Sheet Alloy at 800°, 1000° and 1200°F. Prepared under Grant No. NsG-124-61 (NASA CR-268) for NASA by The University of Michigan, Ann Arbor, July, 1965.
3. Wilson, D. J., Freeman, J. W., and Goodell, P. D.: Sensitivity of the Creep-Rupture Properties of Waspaloy Sheet to Sharp-Edged Notches in the Temperature Range of 1000° - 1400°F. Prepared under Grant No. NsG-124-61 for NASA by The University of Michigan, Ann Arbor, February, 1968.
4. Wilson, D. J., Freeman, J. W., and Goodell, P. D.: Sensitivity of the Creep-Rupture Properties of Nickel-Base Superalloy Sheet to Sharp Edge-Notches in the Temperature Range of 1000° - 1400°F. Prepared under Grant No. NsG-124-61 (NASA CR-1263) for NASA by The University of Michigan, Ann Arbor, January, 1969.
5. Bigelow, W. C., Amy, J. A., and Brockway, L. O.: Electron Microscope Identification of the Gamma Prime Phase of Nickel-Base Alloys. Proc. ASTM, Vol. 56, p. 945, 1956.
6. Larson, F. R., and Miller, J.: A Time-Temperature Relationship for Rupture and Creep Stresses. Trans. Amer. Soc. Mech. Engrs., Vol. 74, p. 765, 1952.
7. Webster, A., and Piercey, B. J.: An Interpretation of the Effects of Stress and Temperature on the Creep Properties of a Nickel-Base Superalloy. Metal Science Journal, Vol. I, p. 97, 1967.
8. Kotval, P. S.: The Microstructure of Superalloys. Metallography, Vol. I, p. 251, 1969.
9. Wolff, U. R.: Orientation and Morphology of $M_{23}C_6$ Precipitated in High-Nickel Austenite. Trans. AIME, Vol. 236, p. 19, 1966.

10. Decker, R. F., and Freeman, J. W.: The Mechanism of Beneficial Effects of Boron and Zirconium on Creep Properties of a Complex Heat Resistant Alloy. Trans. AIME, Vol. 218, p. 277, 1960.
11. Luetjering, G., and Weissmann, S.: Mechanical Properties of Age-Hardened Titanium-Aluminum and Titanium-Copper Alloys. AFML-TR-69-15, 1969.
12. Beardmore, P., Davies, R. G., and Johnston, T. L.: On The Temperature Dependence of the Flow Stress of Nickel-Base Alloys. Trans. of the Metallurgical Society of AIME, Vol. 245, pp. 1537 - 1545, July, 1969.

Table 1

SMOOTH SPECIMEN TENSILE PROPERTIES OF 0.026-INCH THICK WASPALOY SHEET

<u>Heat Treatment</u>	<u>Test Temp. (°F)</u>	<u>Tensile Strength (ksi)</u>	<u>2% Offset Yield Strength (ksi)</u>	<u>Y. S. T. S.</u>	<u>Elong. (%)</u>	<u>R. A. (%)</u>
<u>1/2 hr. 1975°F</u>						
+ 16 hrs. 1400°F	1000	161.0	115.0	0.71	30	32
	1200	167.7	111.3	.67	19	20
	1400	125.0	102.0	.82	6	16
<u>1/2 hr. 1975°F</u>						
+ 10 hrs. 1700°F	1000	148.5	94.9	.64	32	28
	1200	145.0	91.0	.63	26	25
	1400	115.0	92.0	.80	15	23

Table 2

SMOOTH SPECIMEN TENSILE AND CREEP-RUPTURE PROPERTIES
OF 0.026-INCH THICK WASPALOY

Test Temp (°F)	Stress (ksi)	Rupture Time (hrs.)	Elong. (%)	R. A. (%)	Min. Creep Rate (%/hour)	Intergranular Crack Length (%)
<u>Material Solution Treated 1/2 hour at 1975°F and Aged 16 hours at 1400°F</u>						
1000	161*	Tensile	30	32	-	0
	150	131.9	15.0	23	.017	4
	145	207.6	13.5	20	.00525	6
	135*	517.0	7.0	14	.00050	8
	130	In Progress			.00009	
1100	135	83.1	4.7	12	.0025	10
	120	1461.2	2.5	12	.00016	14
	120	1047.6	2.8	12	.0003	19
1200	167.7	Tensile	19.5	20	-	0
	120	3.6	4.3	13	-	8
	90*	376.5	1.5	9	.00045	23
	80	1240.8	2.2	10	.000096	34
1300	80*	63.7	1.7	7	.005	48
	65	302.4	1.8	7	.00060	50
	55	1288.5	5.1	10	.00038	60
1400	125*	Tensile	5.8	16	-	8
	65	18.1	2.8	9	-	38
	45	406.1	6.5	11	.0025	44
	38*	1006.9	8.1	15	.00053	
<u>Material Solution Treated 1/2 hour at 1975°F and Aged 10 hours at 1700°F</u>						
1000	148.5*	Tensile	32.4	28	-	0
	140	82.7	23.8	22	-	1
	125*	566.5	14.3	15	.0027	7
1100	125	36.4	17.5	17	.0650	2
	100	366.2	6.8	12	.0028	16
1200	145	Tensile	26.5	26	-	0
	100	38.7	7.5	12	.0692	17
	80*	1870.1	5.4	11	.00018	32
1300	100	7.9	8.4	12	-	11
	80	52.6	5.6	11	-	28
	60	671.1	7.6	10	.00112	38
	38.5	In Progress			.000062	
1400	115*	Tensile	14.9	23	-	12
	60	35.0	12.0	15	-	30
	38*	931.1	9.0	14	.0011	52
	26.6	In Progress			.000152	

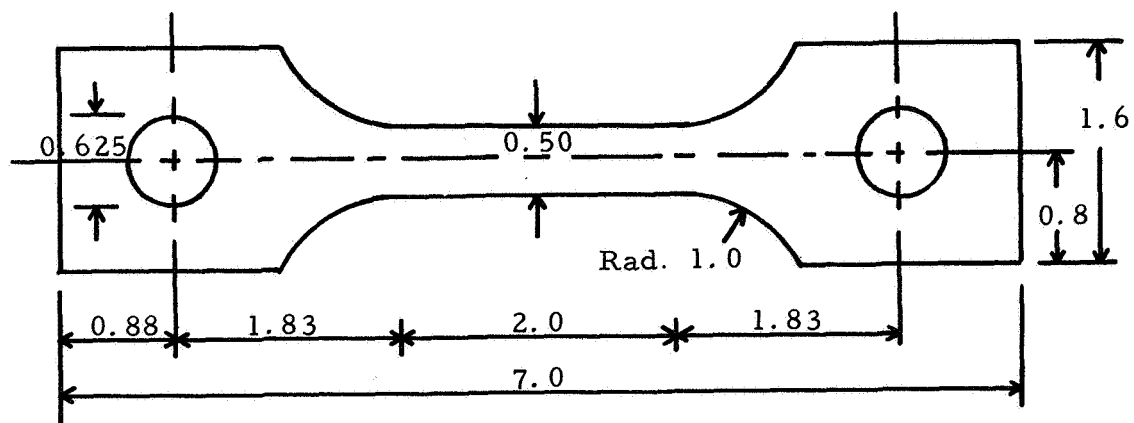


Figure 1 Smooth (unnotched) Specimen ($K_t=1.0$)

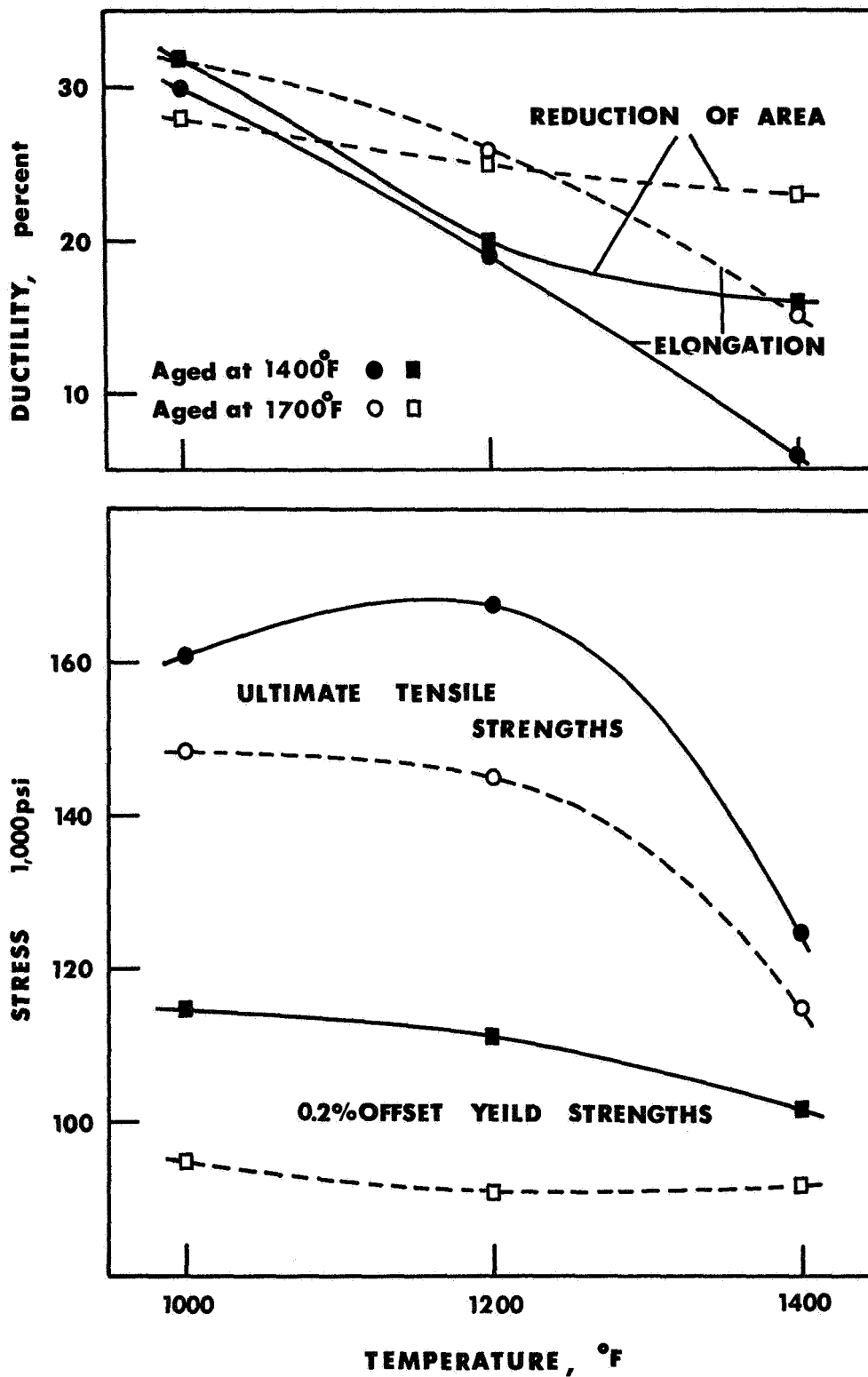
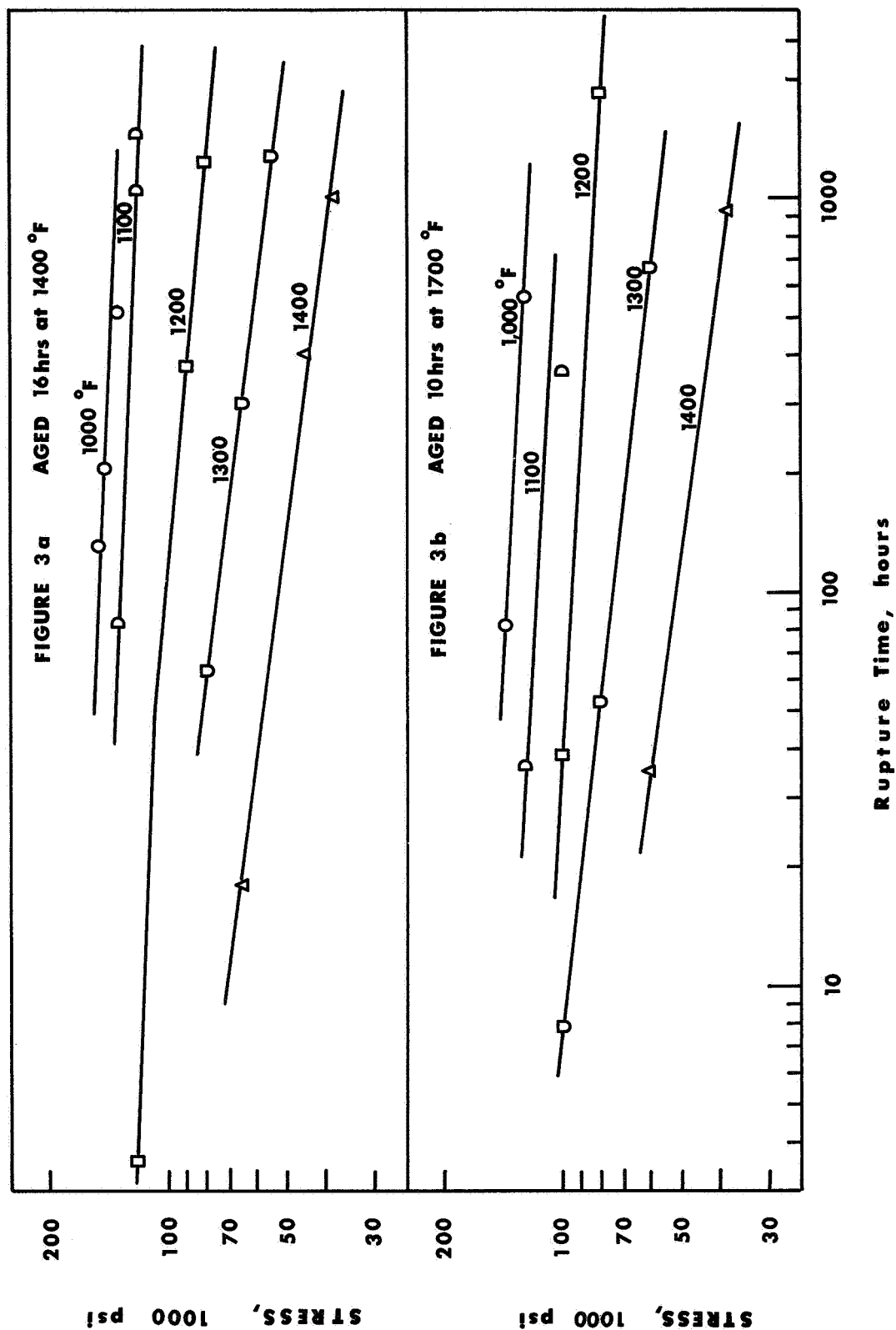


Figure 2 Smooth specimen tensile properties from 1000° - 1400°F for 0.026-inch thick Waspaloy sheet heat treated 1/2 hour at 1975°F and aged 16 hours at 1400°F or 10 hours at 1700°F



Figures 3a, b Stress versus rupture time data obtained from smooth specimens of 0.026-inch thick Waspaloy sheet heat treated 1/2 hour at 1975°F and aged.

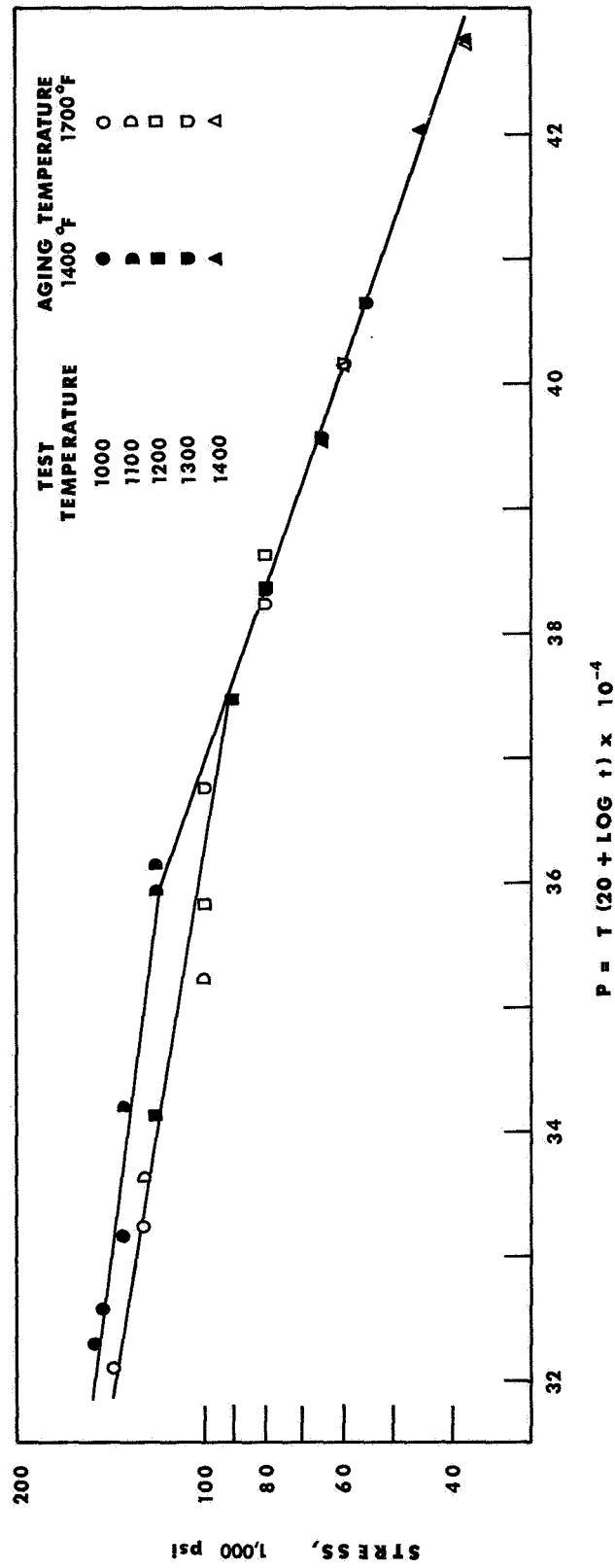
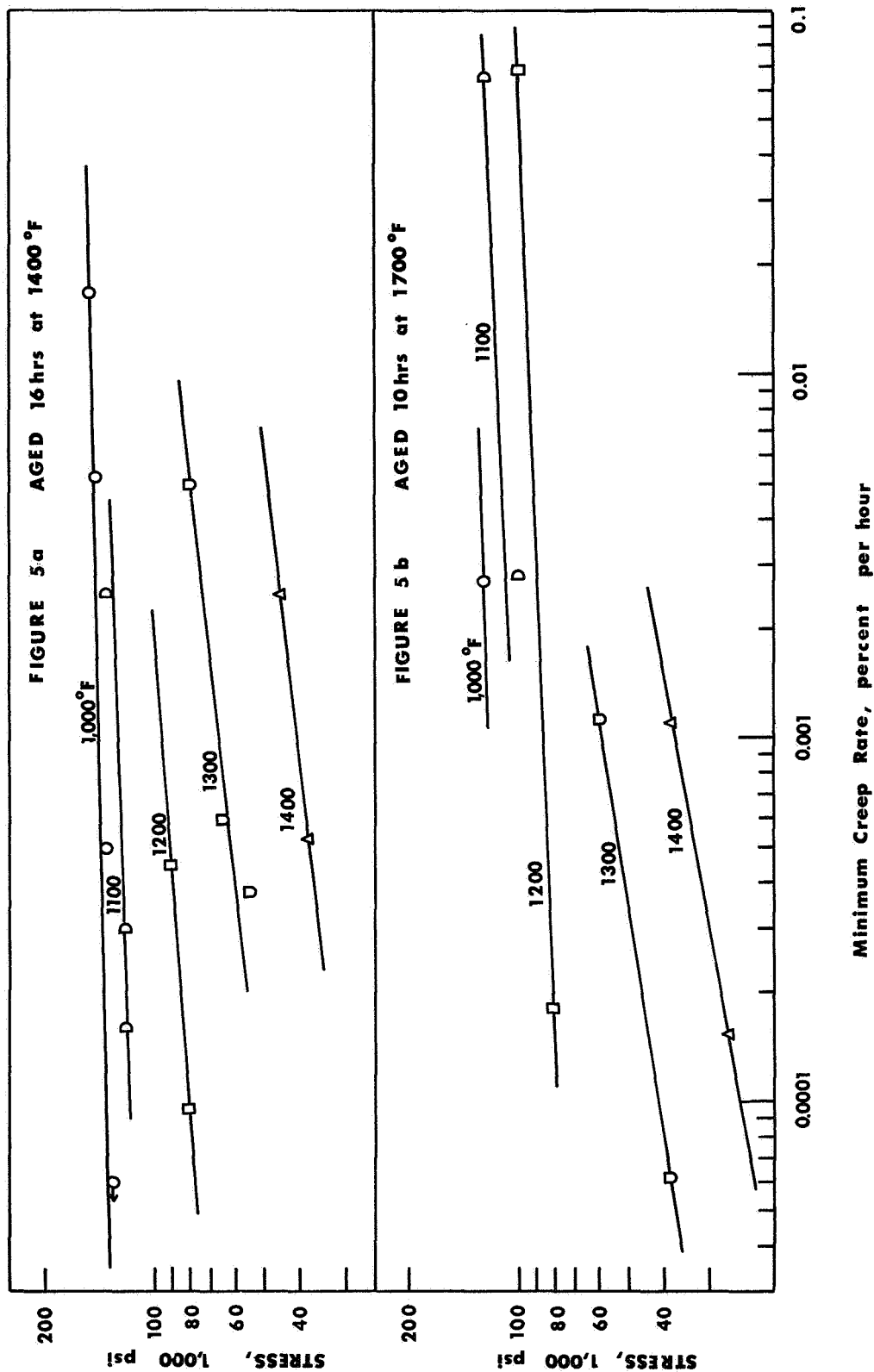


Figure 4 Time-temperature dependence of the rupture strengths at 1000° - 1400°F of smooth specimens of 0.026-inch thick Waspaloy sheet heat treated 1/2 hour at 1975°F and aged 16 hours at 1400°F or 10 hours at 1700°F.



Figures 5a, b Stress versus minimum creep rate at 1000° - 1400°F for 0.026-inch thick Waspaloy sheet heat treated 1/2 hour at 1975°F and aged at 1400°F or at 1700°F.

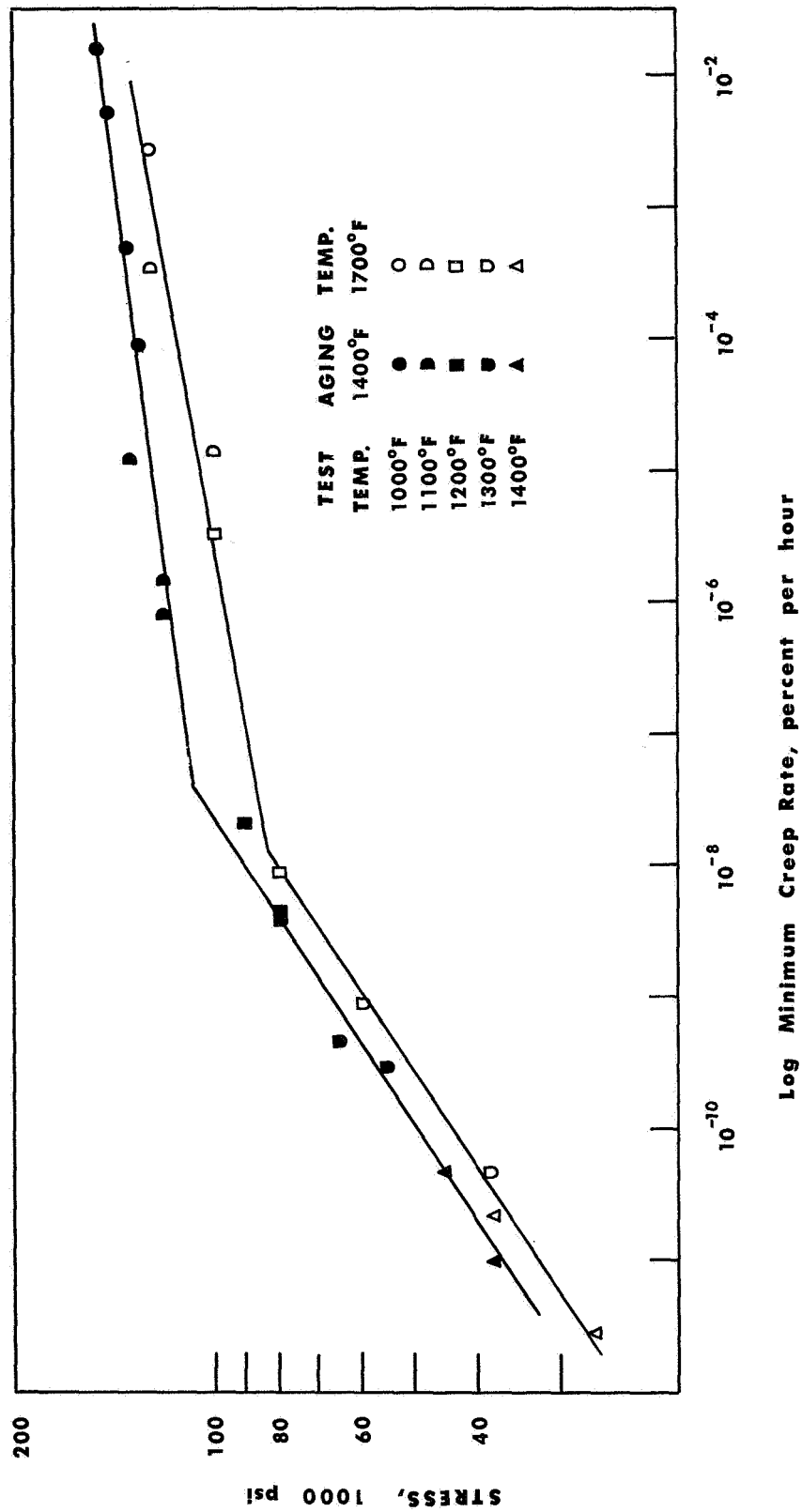


Figure 6 Stress versus minimum creep rates temperature compensated to 1000°F from tests at 1000° - 1400°F for 0.026-inch thick Waspaloy sheet heat treated 1/2 hour at 1975°F and aged 16 hours at 1400°F or 10 hours at 1700°F.

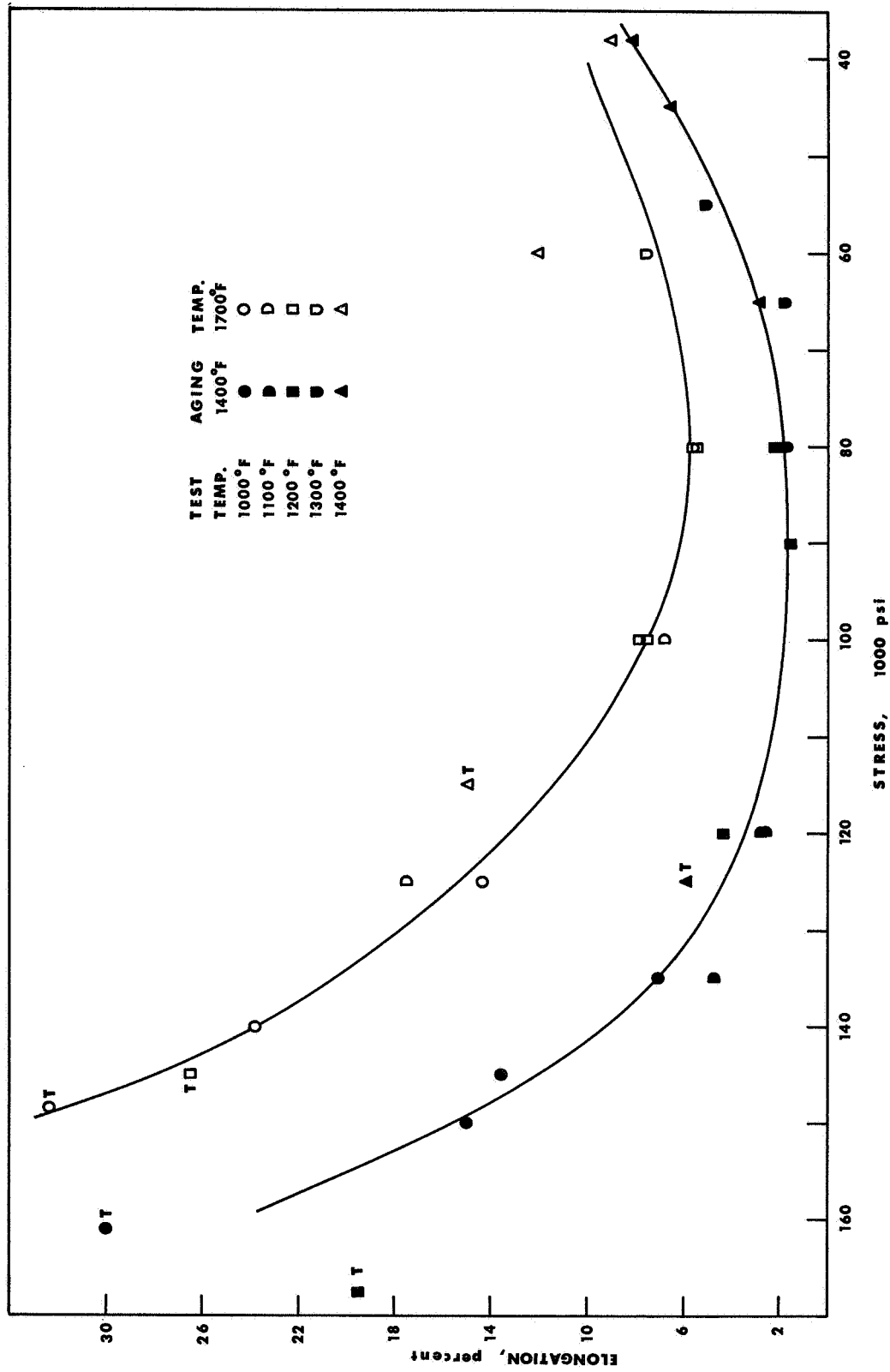


Figure 7 Elongation at fracture versus stress for tensile (designated T) and rupture tests at 1000° - 1400°F for 0.026-inch thick Waspaloy sheet heat treated 1/2 hour at 1975°F and aged 16 hours at 1400°F or 10 hours at 1700°F.

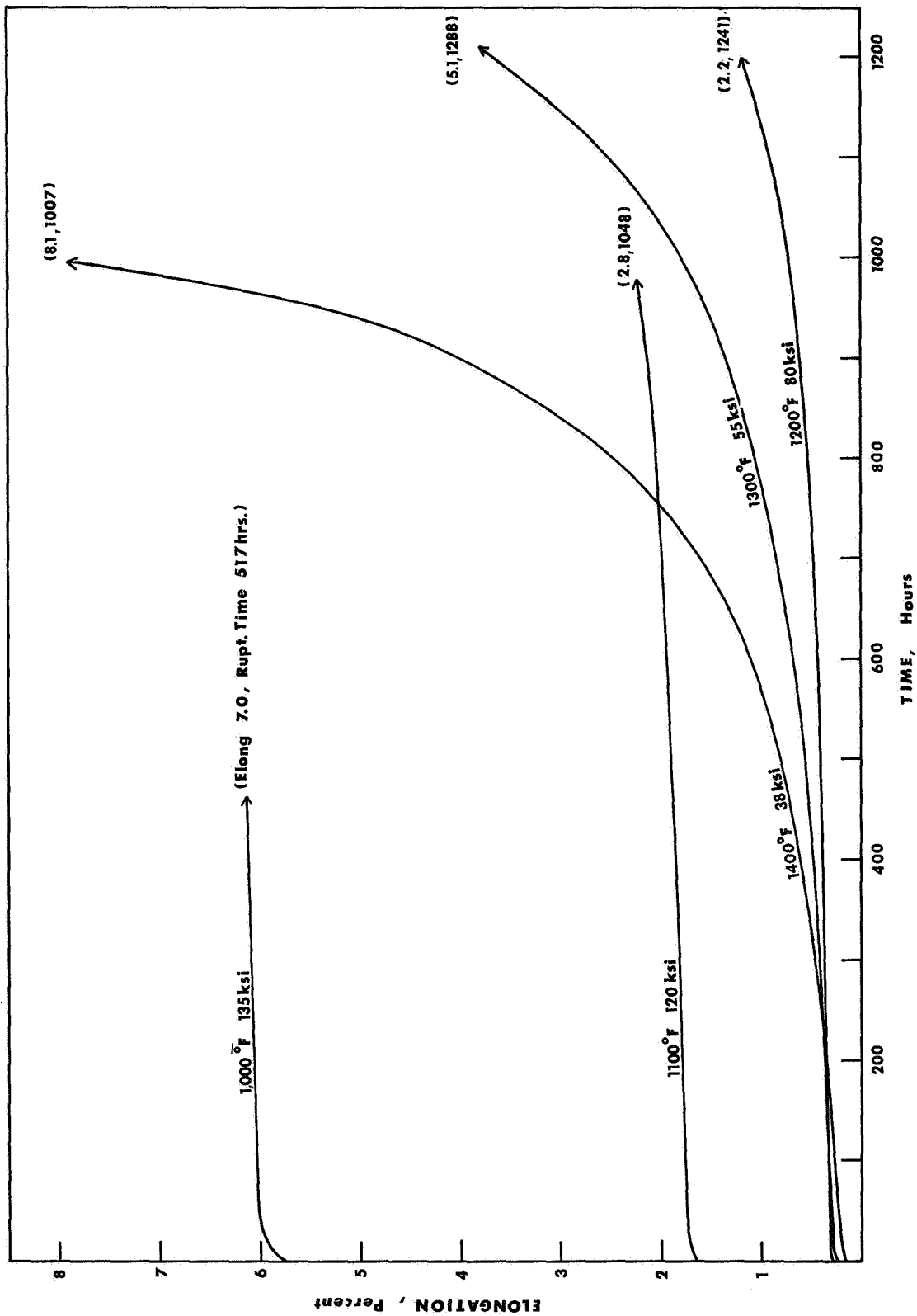


Figure 8 Selected creep curves obtained at 1000° - 1400°F for 0.026-inch thick Waspaloy sheet heat treated 1/2 hour at 1975°F and aged 16 hours at 1400°F. Bracketed values indicate the rupture elongation and time.

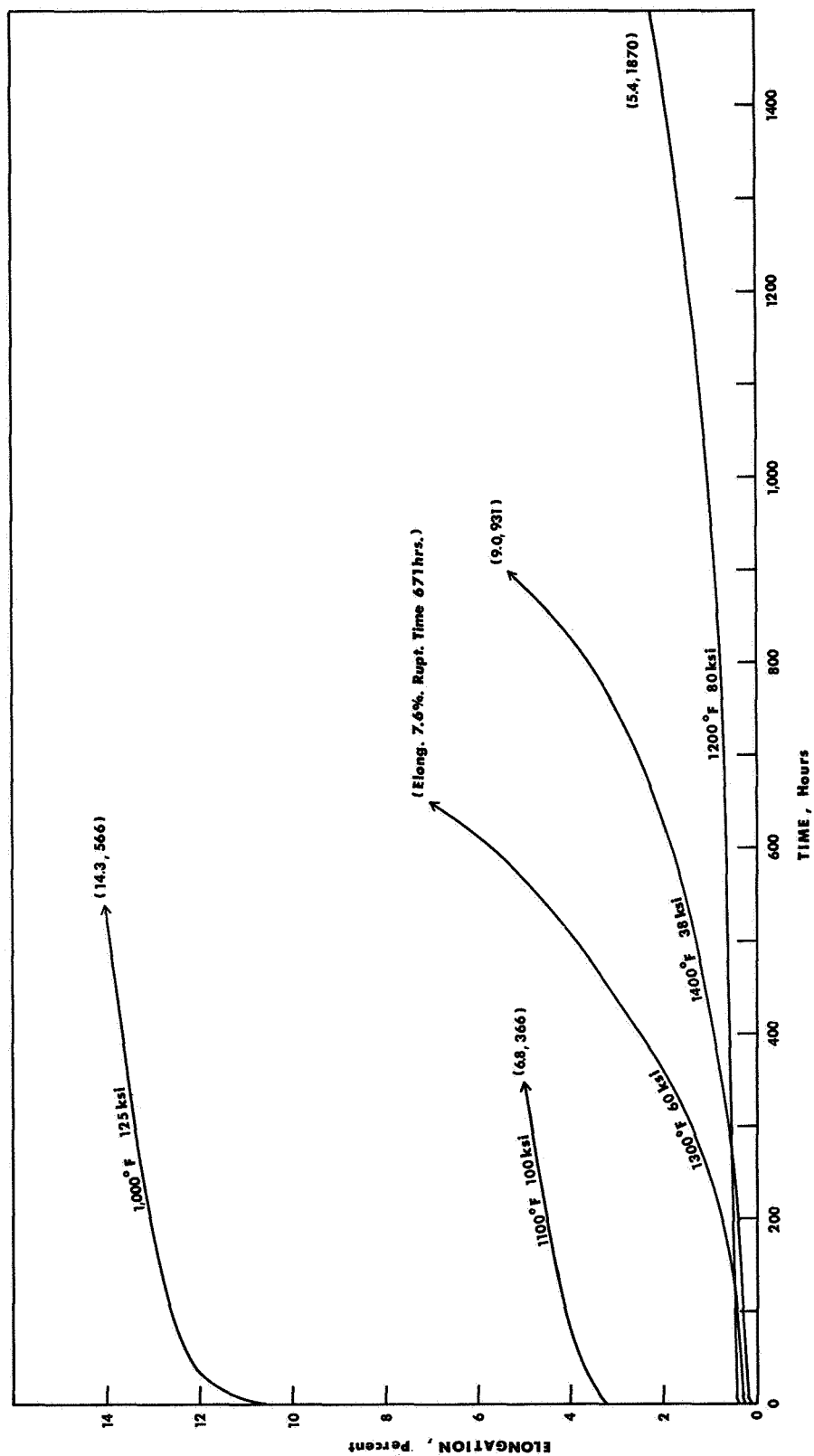


Figure 9 Selected creep curves obtained at 1000° - 1400°F for 0.026-inch thick Waspaloy sheet heat treated 1/2 hour at 1975°F and aged 10 hours at 1700°F. Bracketed values indicate the rupture elongation and times.

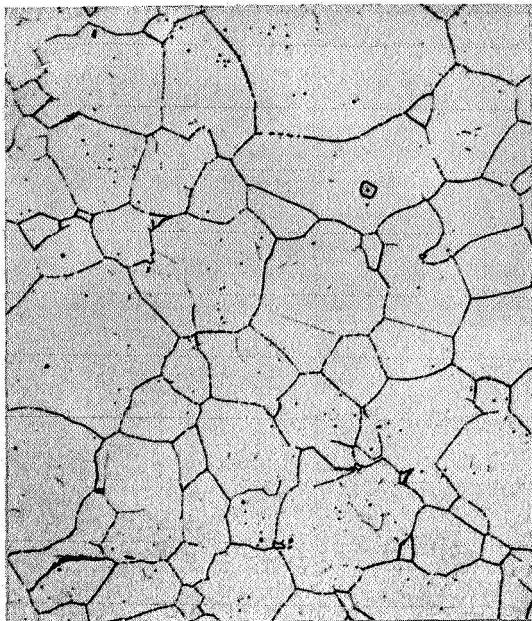


Figure 10a

X500

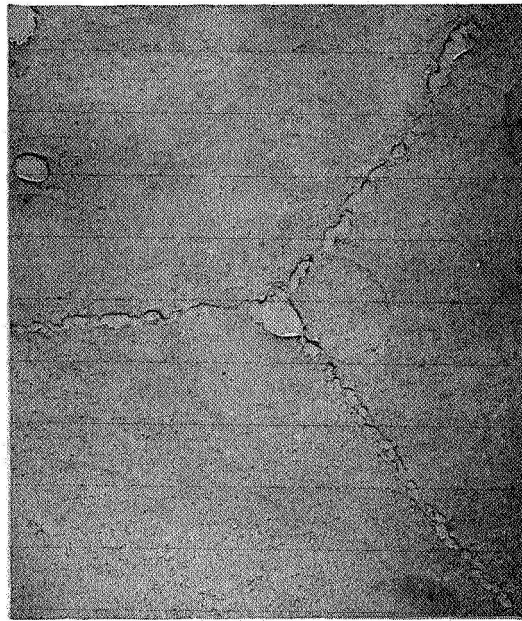


Figure 10b

X5,400

Aged 16 hours at 1400°F

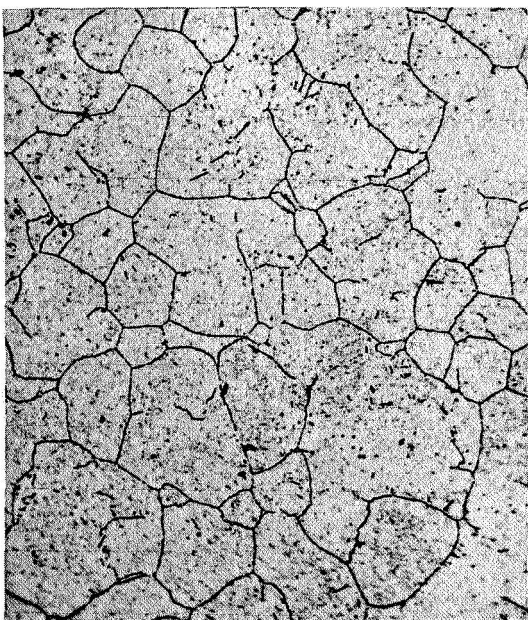


Figure 10c

X500



Figure 10d

X5,400

Aged 10 hours at 1700°F

Figure 10. - Photomicrographs of 0.026-inch thick Waspaloy sheet heat treated 1/2 hour at 1975°F and aged.

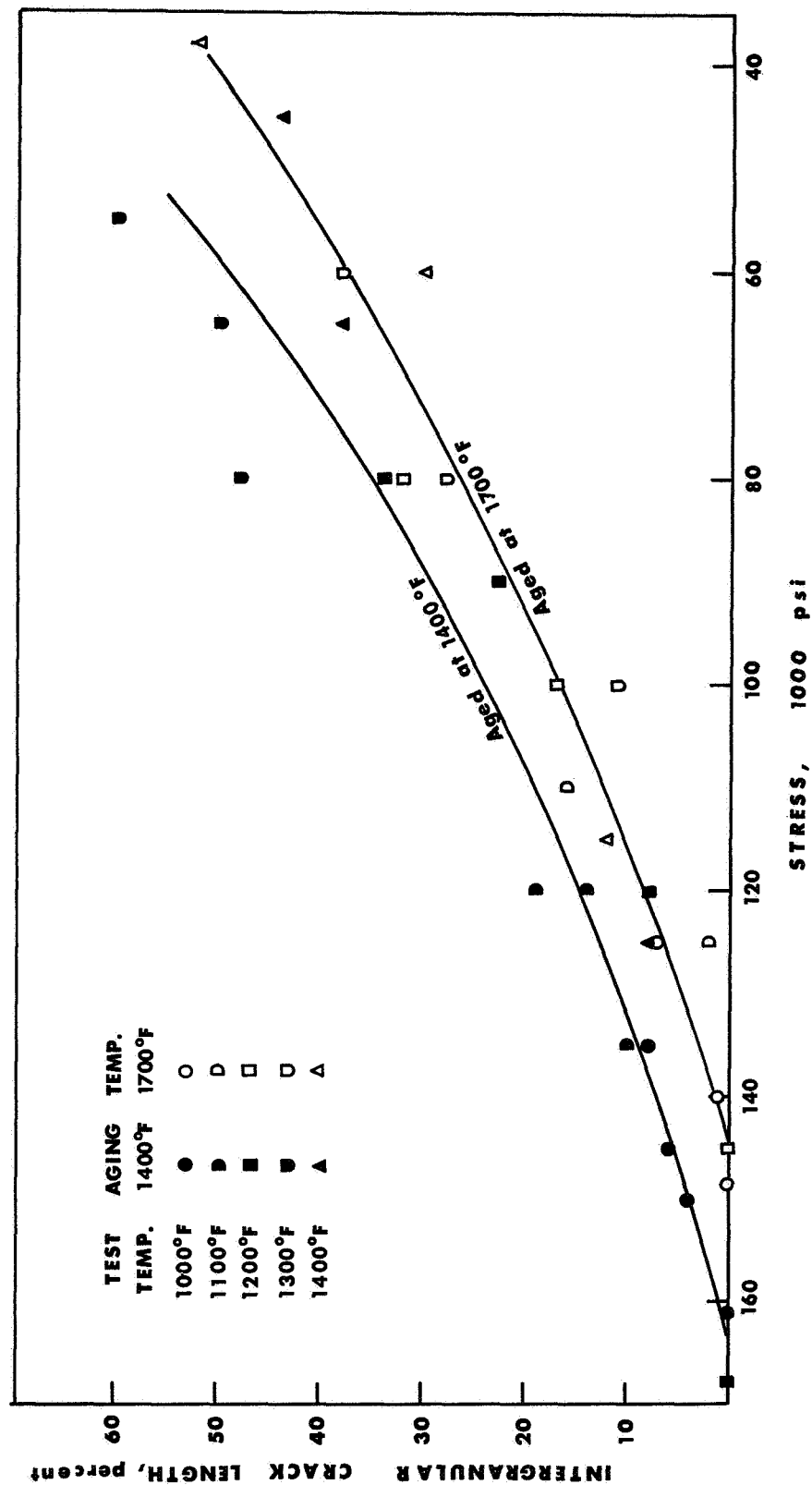


Figure 11 Intergranular crack length versus initial loading stress at 1000° - 1400°F obtained from fractured tensile and rupture tested smooth specimens of 0.026-inch thick Waspaloy sheet heat treated 1/2 hour at 1975°F and aged 16 hours at 1400°F or 10 hours at 1700°F.

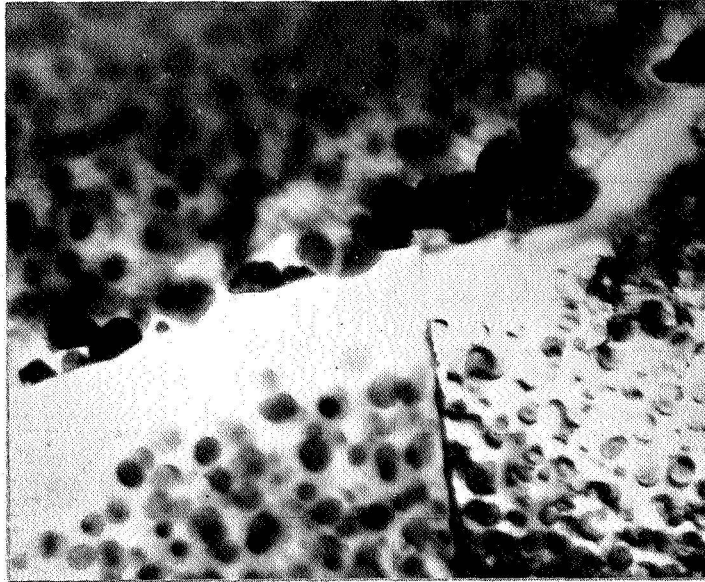


Figure 12a

X35,000

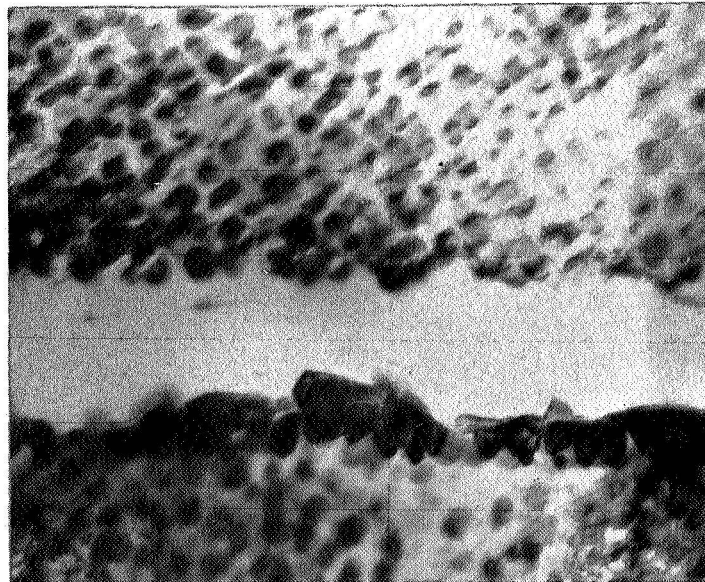


Figure 12b

X27,000

Transmission electron micrographs of Waspaloy, heat treated 1/2 hour at 1975°F, aged, and creep rupture tested at 38 ksi at 1400°F. The zones denude of the γ' precipitate formed during the creep exposure. (Figure 12a- Aged 16 hours at 1400°F, ruptured in 1007 hours; Figure 12b- Aged 10 hours at 1700°F, ruptured in 931 hours.)

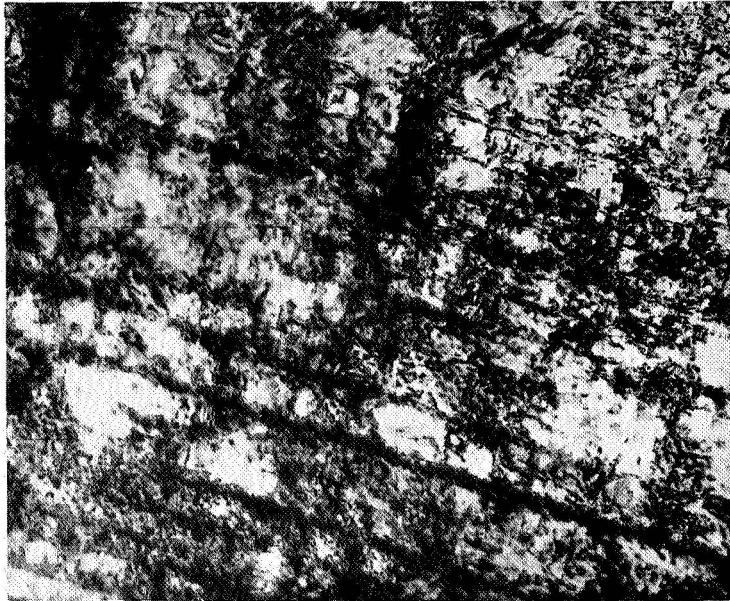


Figure 13a

X24,000

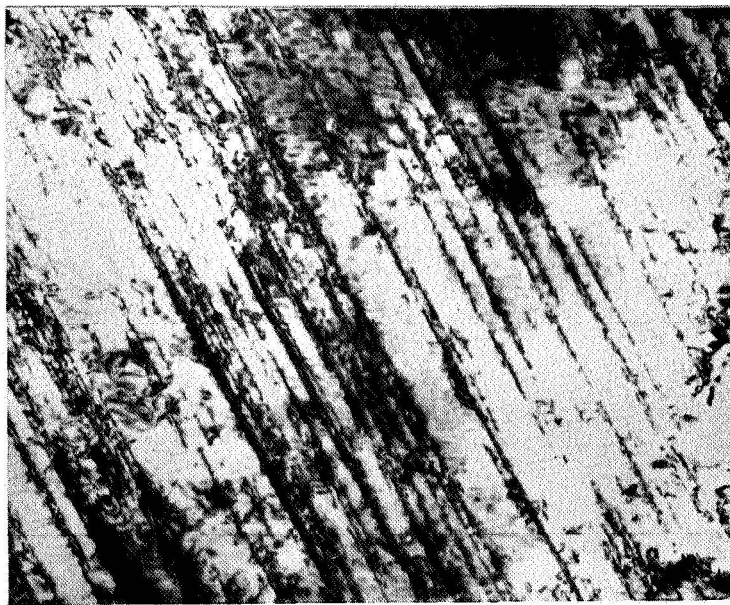


Figure 13b

X49,000

Thin-foil electron micrographs of Waspaloy, heat treated 1/2 hour at 1975°F, aged 16 hours at 1400°F and tensile tested at 1000°F (YS = 115 ksi, TS = 161 ksi, Elong. = 30%). The structure is highly deformed in particular on (111) slip planes.

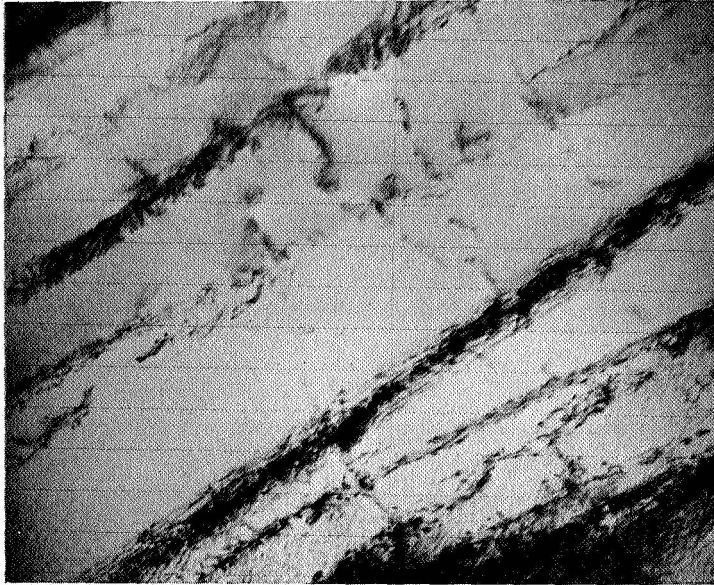


Figure 14a

X27,000

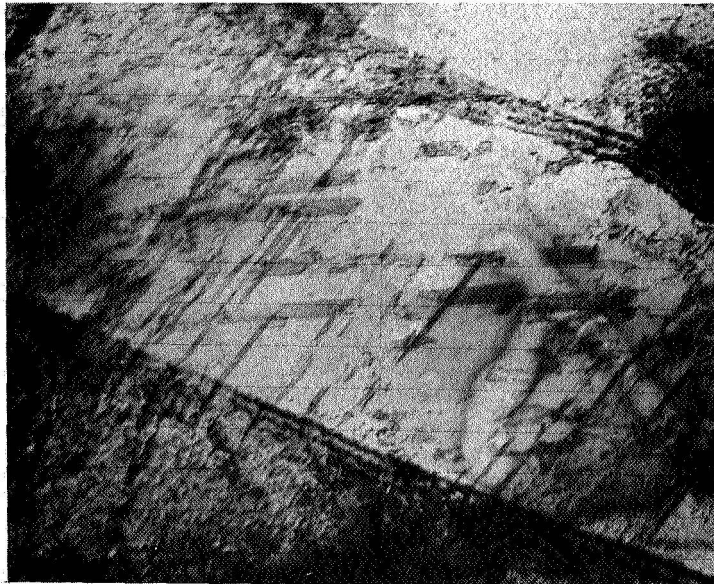


Figure 14b

X22,000

Thin-foil electron micrographs of Waspaloy, heat treated 1/2 hour at 1975°F, aged 16 hours at 1400°F and creep rupture tested at 135 ksi at 1000°F (ruptured in 517 hours at 7.0% elongation). Deformation is concentrated on (111) slip planes. Stacking faults, associated with extended dislocations, are also evident.

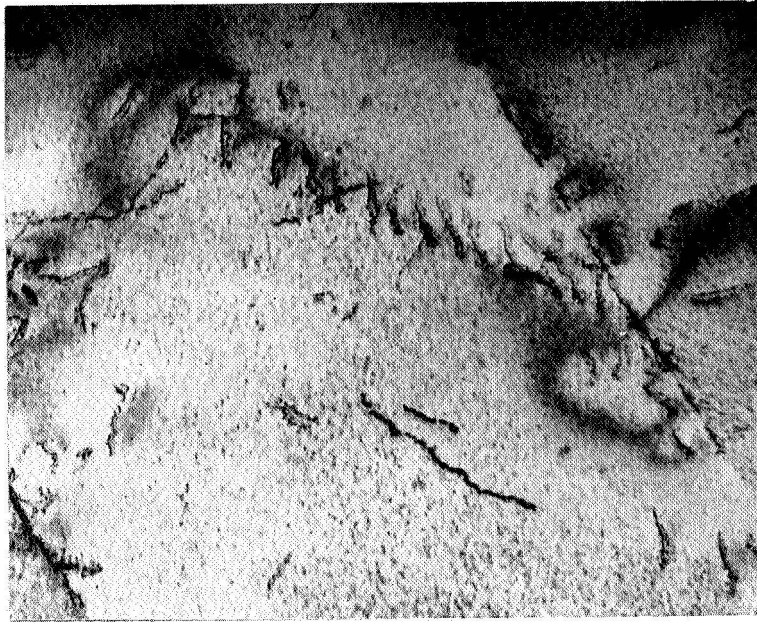


Figure 15a

X42,000

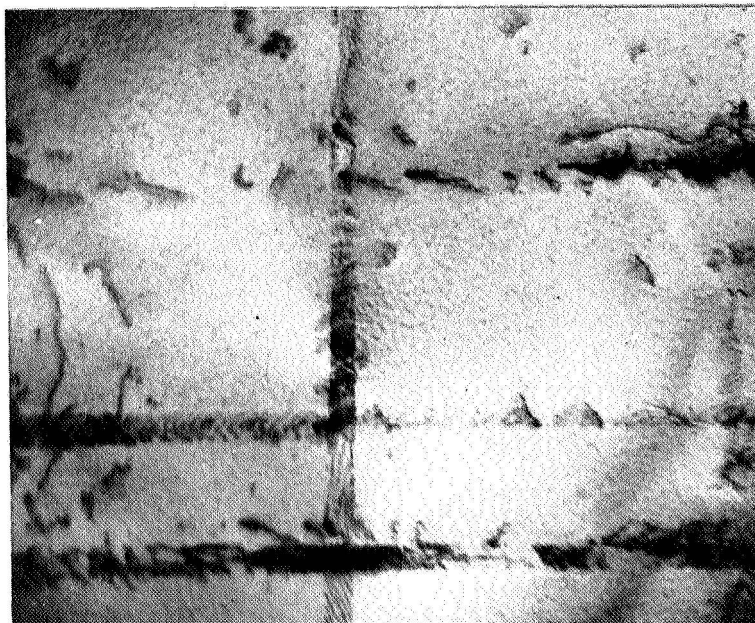


Figure 15b

X22,000

Transmission electron micrographs of Waspaloy, heat treated 1/2 hour at 1975°F, aged 16 hours at 1400°F and strained 2.3% at 1000°F. Dislocations are present in pile ups and are frequently "paired" to form superdislocations.

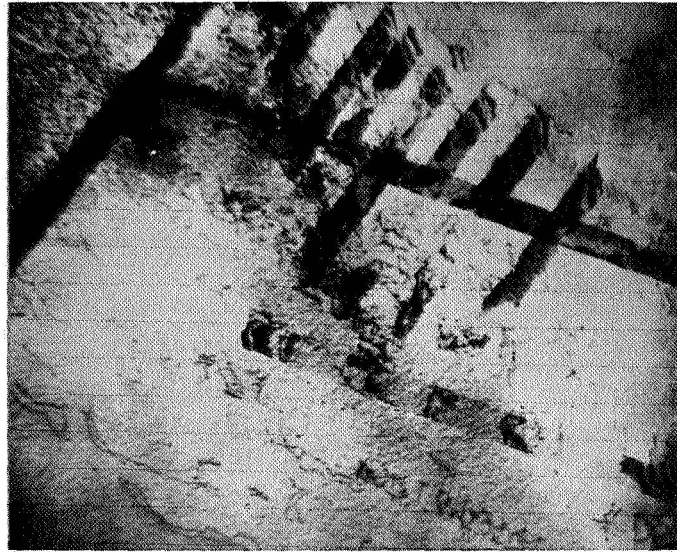


Figure 16a

X11,000



Figure 16b

X13,000



Figure 16c

X19,000

Thin-foil electron micrographs of Waspaloy, heat treated 1/2 hour at 1975°F, aged 16 hours at 1400°F and creep rupture tested at 1200° and 1300°F. Dislocations are present in pile ups and are in the main extended to form stacking fault ribbons. (Figures 16a, b - tested at 90 ksi and 1200°F, ruptured in 376 hours at 1.5% elongation; Figure 16c- tested at 80 ksi at 1300°F, ruptured in 64 hours at 1.7% elongation.)

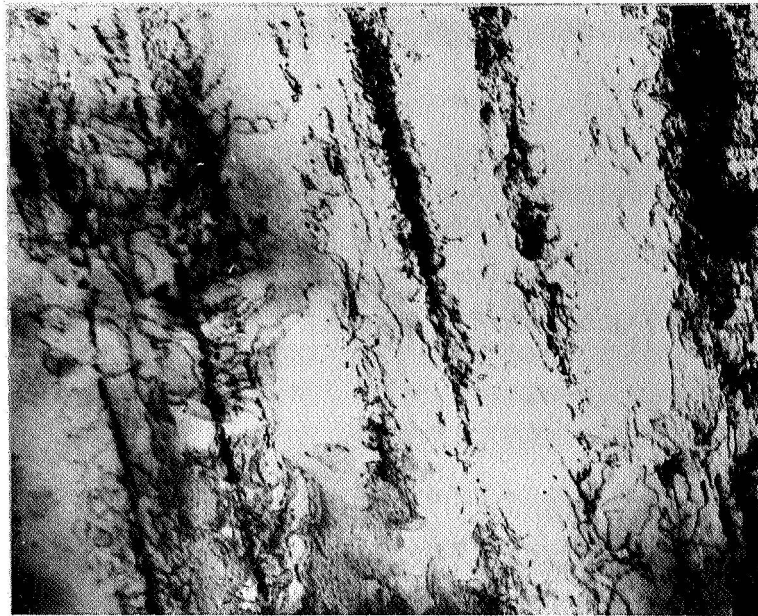


Figure 17a

X18,000

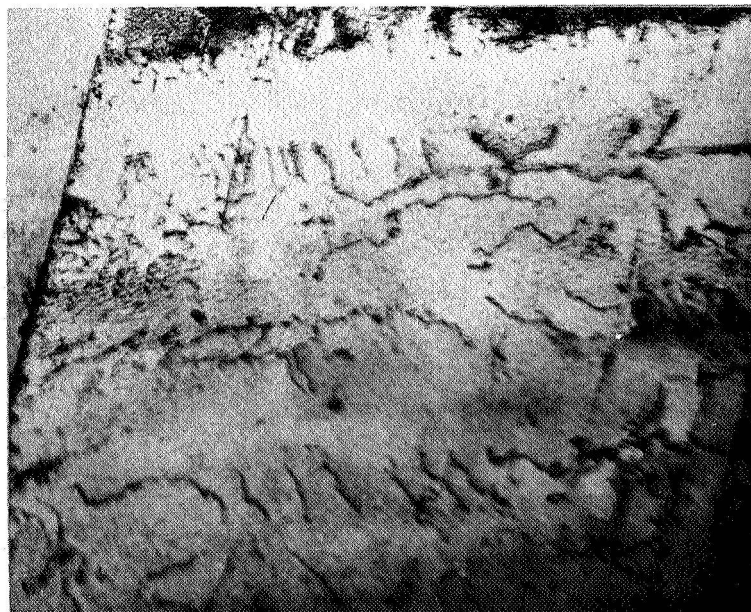


Figure 17b

X20,000

Thin-foil electron micrographs of Waspaloy, heat treated 1/2 hour at 1975°F, aged 16 hours at 1400°F and tensile tested at 1400°F (YS = 102 ksi, TS = 125 ksi, Elongation = 6%).

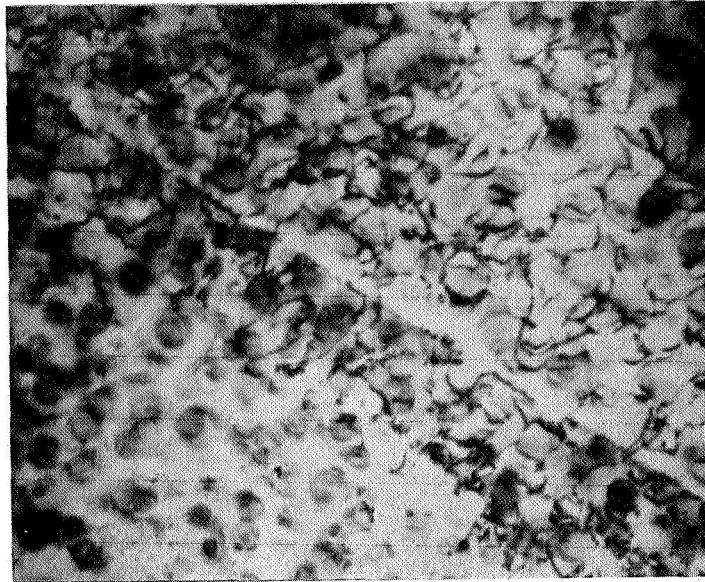


Figure 18a

X67,000

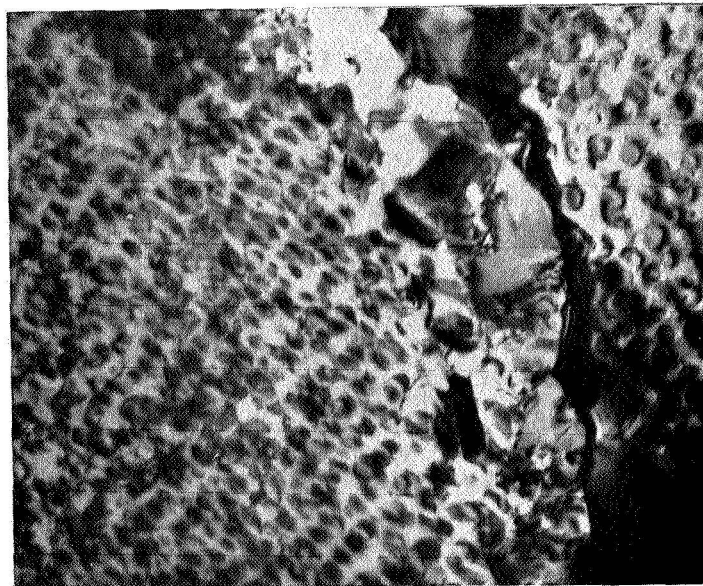


Figure 18b

X56,000

Transmission electron micrographs of Waspaloy, heat treated 1/2 hour at 1975°F, aged 16 hours at 1400°F and creep-rupture tested at 38 ksi at 1400°F (ruptured in 1007 hours at 8.1% elongation). The γ' particles increased in size from approximately 75Å to 900Å during the test exposure. The deformation evident in Figure 18a is homogeneous. Contrast effects associated with coherent γ' are present in Figure 18b.

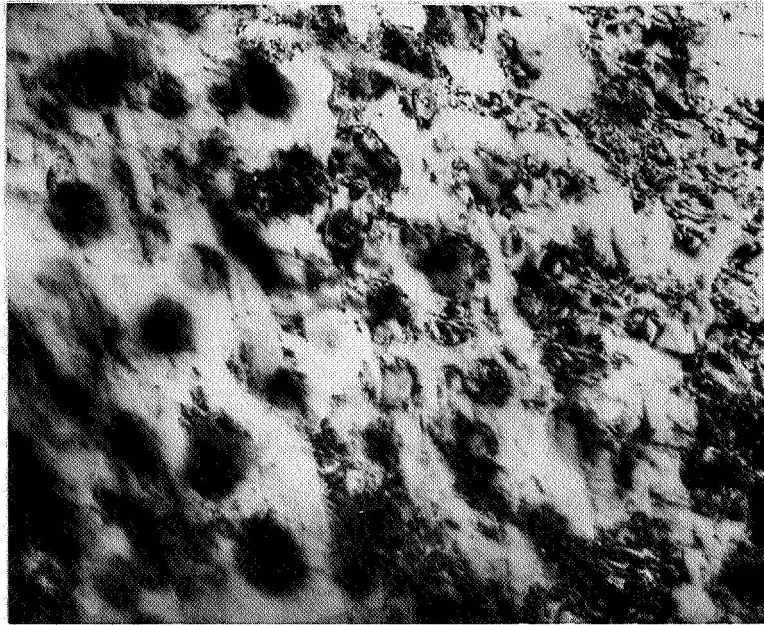


Figure 19a

X75,000



Figure 19b

X51,000

Transmission electron micrographs of Waspaloy, heat treated 1/2 hour at 1975°F, aged 10 hours at 1700°F and tensile tested at 1000°F (YS = 95 ksi, TS = 148 ksi, Elongation = 32%). The structures are highly deformed with a tendency for the deformation to be maximized on slip planes.

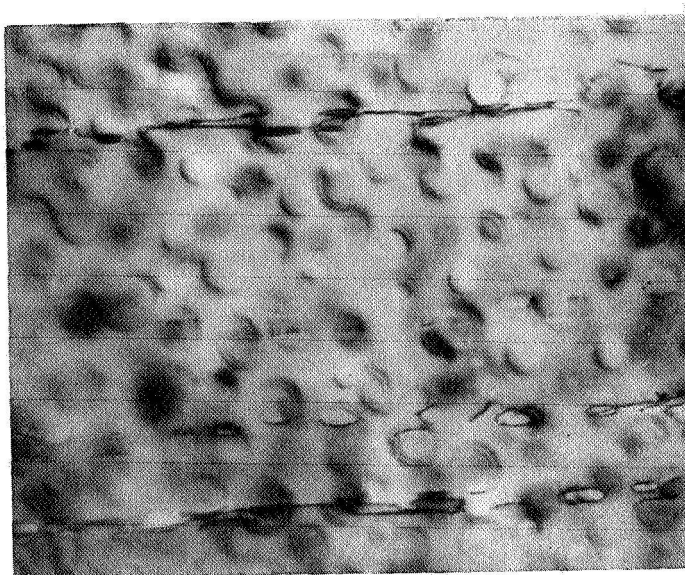


Figure 20a

X51,000

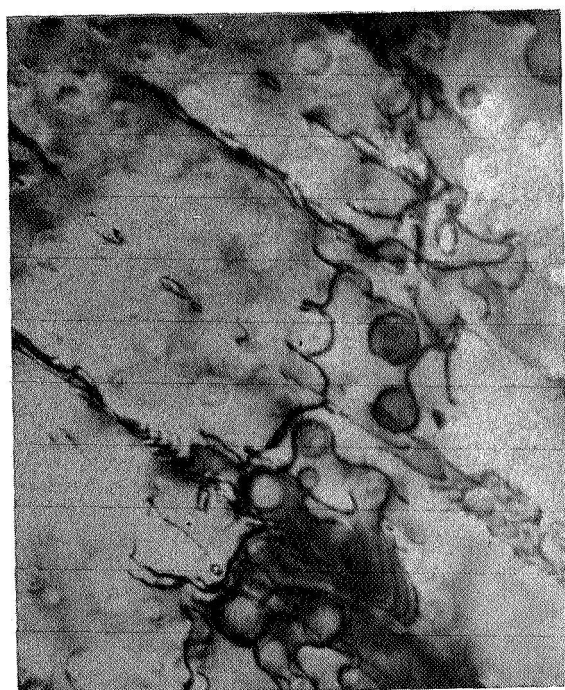


Figure 20b

X47,000

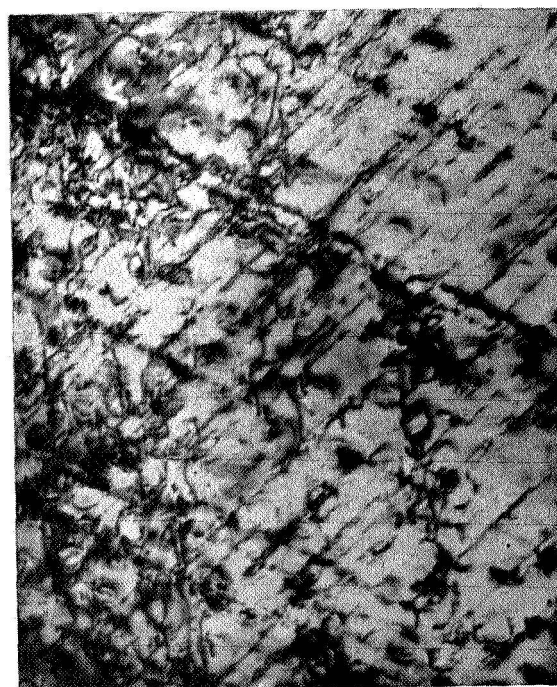


Figure 20c

X38,000

Thin-foil electron micrographs of Waspaloy, heat treated 1/2 hour at 1975°F, aged 10 hours at 1700°F and strained approximately 1, 2.5, and 6% at 1000°F (Figures 20a, b & c respectively). Dislocation can be observed bowing between γ' particles leaving 'pinched off' dislocation loops around the particles. At the high strain level the deformation, although generally "homogeneous," does tend to be concentrated on (111) slip planes.

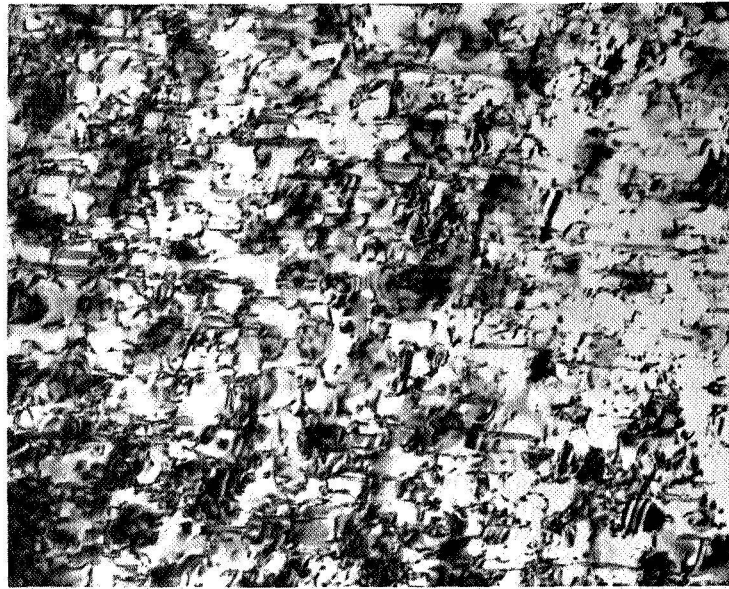


Figure 21a

X55,000

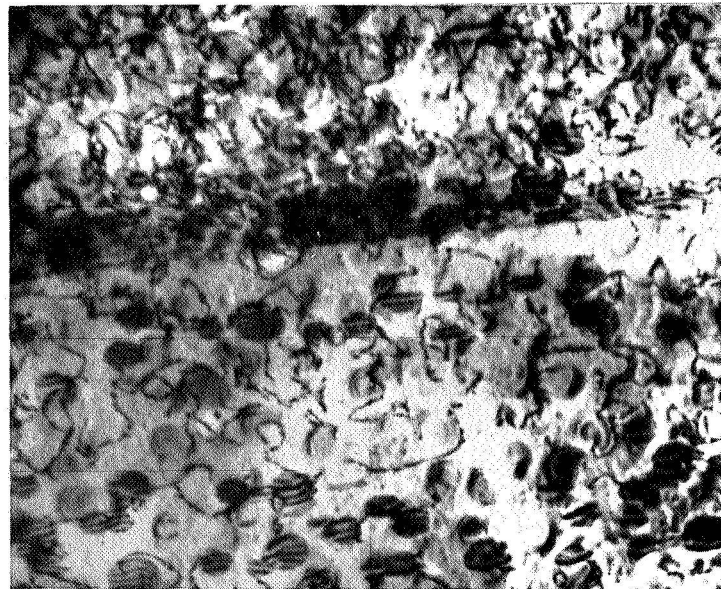


Figure 21b

X50,000

Thin-foil electron micrographs of Waspaloy, heat treated 1/2 hour at 1975°F, aged 10 hours at 1700°F and creep-rupture tested at 1000° and 1200°F. The deformation is "homogeneous." Microtwins are present in Figure 21a while dislocation loops about γ' particles are evident in Figure 21b. (Figure 21a - tested at 125 ksi at 1000°F, ruptured in 566 hours at 14.3% elongation; Figure 21b - tested at 80 ksi at 1200°F, ruptured in 1870 hours at 5.4% elongation.)

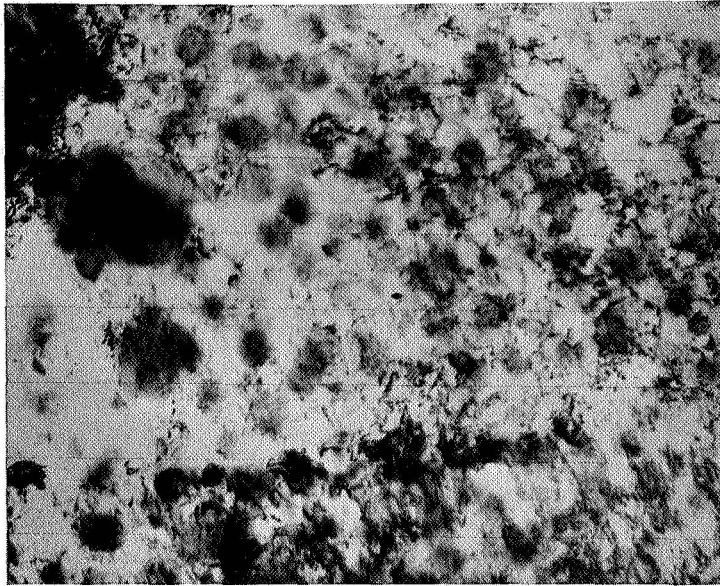


Figure 22a

X43,000

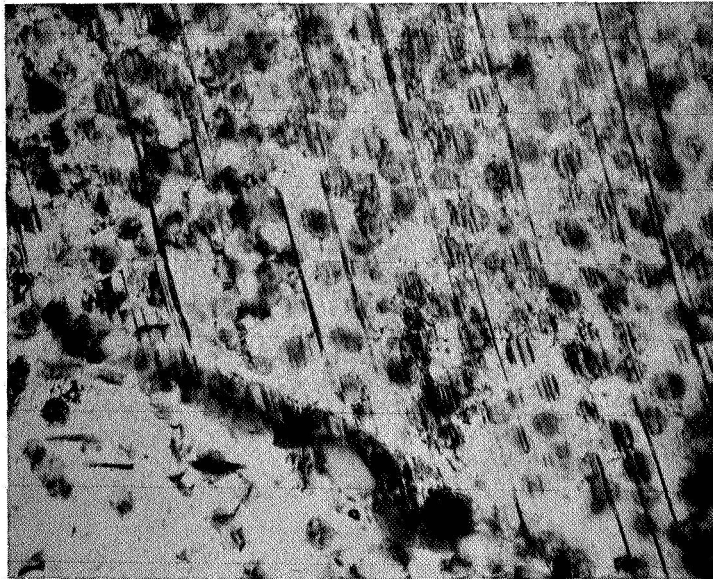


Figure 22b

X38,000

Thin-foil electron micrographs of Waspaloy, heat treated 1/2 hour at 1975°F, aged 10 hours at 1700°F and tensile tested at 1400°F (YS = 92 ksi, TS = 115 ksi, Elongation = 15%). The dislocations are "homogeneously" distributed in Figure 22a. In areas of Figure 22b microtwins are apparently confined to the γ' precipitate particles.

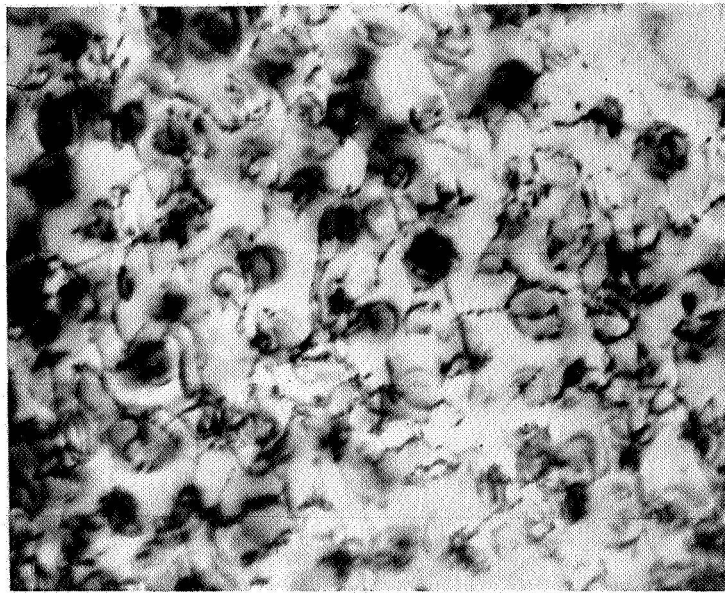


Figure 23a

X33,000

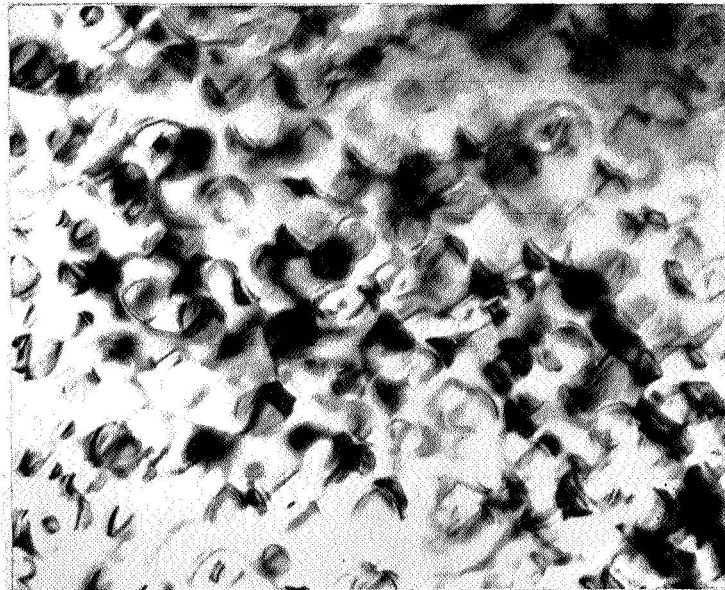


Figure 23b

X36,000

Transmission electron micrographs of Waspaloy, heat treated 1/2 hour at 1975°F, aged 10 hours at 1700°F and creep-rupture tested at 38 ksi at 1400°F (ruptured in 931 hours at 9% elongation). The γ' particles increased in size from about 1000Å to 1500Å during the test exposure. A "homogeneous" distribution of dislocations is evident in Figure 23a, while in Figure 23b contrast effects due to coherent γ' particles are discernable.